Diagnostics Developments

EURATOM - IPPLM Association, Warsaw, Poland

presented by M. Scholz

Outline

1. Gas Electron Multiplier Detector for X-ray Crystal Spectrometry
2. Diamond detectors to detect escaping fast alpha particles
3. Study of $LaBr_3$:Ce, $CeBr_3$ and NaI(Tl) Scintillators for Gamma Camera for Plasma Diagnostic in Tokamaks
4. Gateable MCP based Camera for VUV and Soft X-ray Imaging of Magnetically Confined Plasma

Gas Electron Multiplier Detector for X-ray Crystal Spectrometry

M. Chernyshova, T. Czarski, W. Dominik,
K. Jakubowska, L. Karpinski, G. Kasprowicz,
K. Pozniak, J. Rzadkiewicz, M. Scholz, W. Zabolotny

Institute of Plasma Physics and Laser Microfusion, Warsaw,
Warsaw University, Faculty of Physics, Institute of Experimental Physics,
Warsaw University of Technology, Institute of Electronic Systems,
Institute of Nuclear Physics of the Polish Academy of Sciences, Kraków

KX1 – x-ray crystal spectrometr

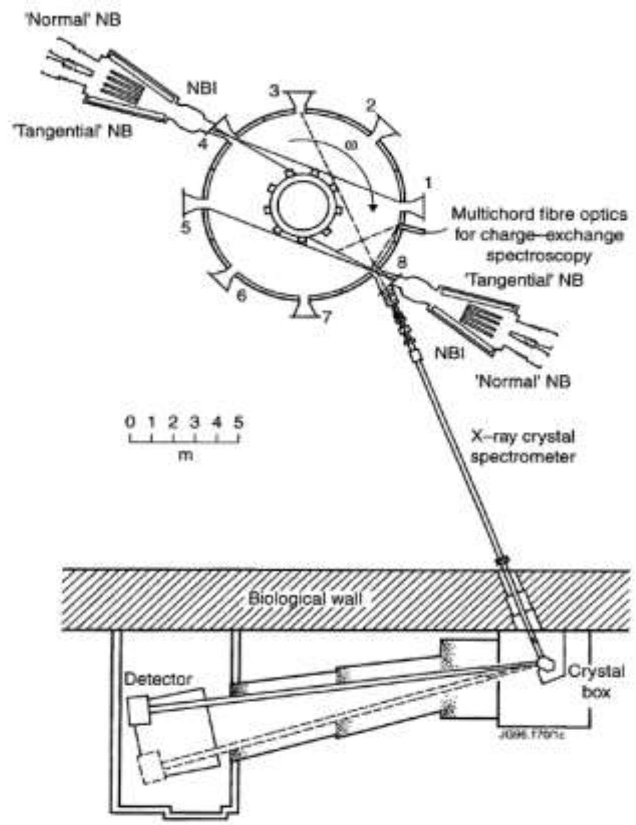

Horizontal cross-section of the x-ray crystal spectrometer (KX1) on the JET tokamak

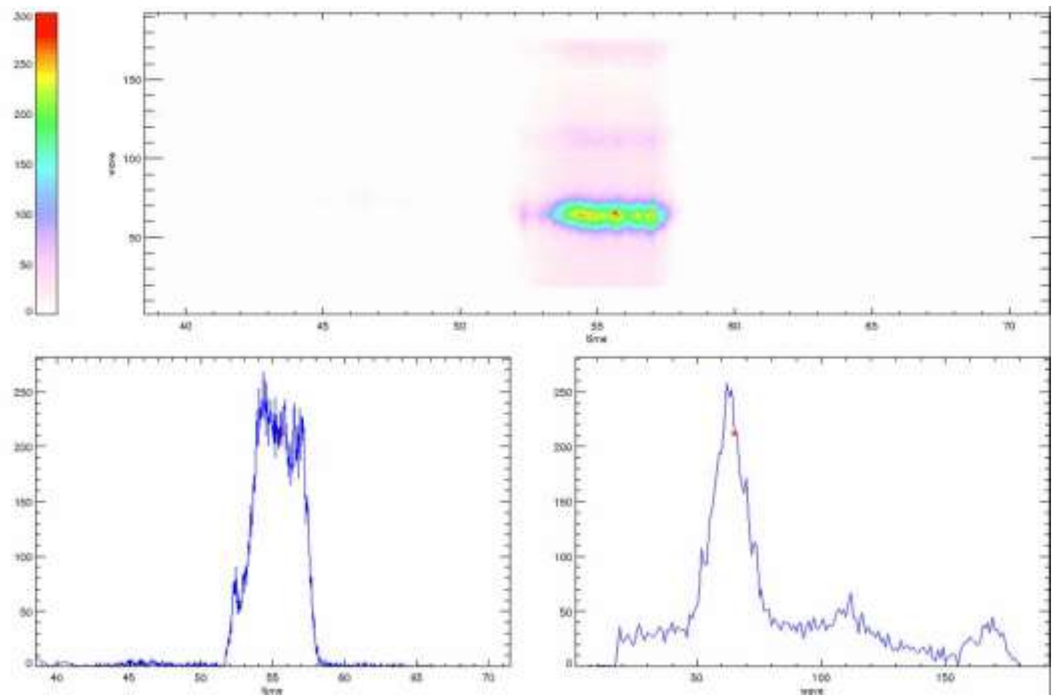

X-ray spectra of Ni monitored by previous KX1 diagnostics on JET discharge no #61098. Time evolution of counting rates for all 196 detector strips (upper part), time evolution of the counting rate for a single strip (bottom left) and a single 30 ms-high-resolution x-ray spectrum (bottom right).

KX1 – old and new detectors

- KX1 monitored all three orders together - without energy resolution.
- The continuum radiation from higher orders of reflection was neglected.
- Therefore it was not possible to obtain information about continuum radiation in different reflection orders (energy ranges)

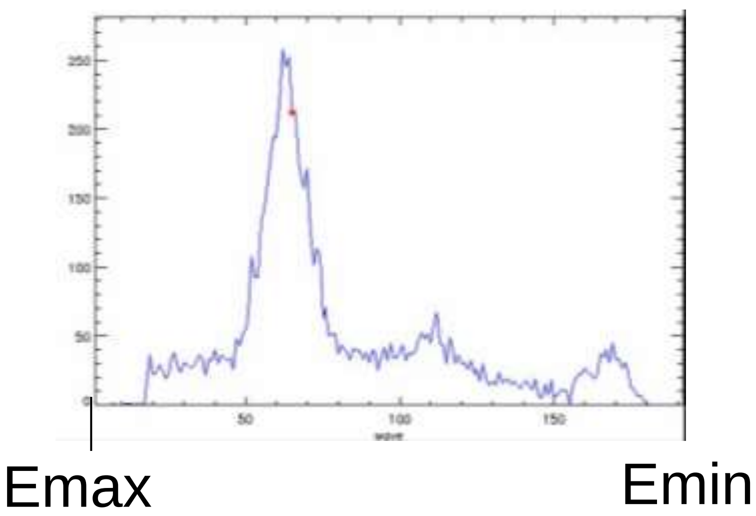

It will monitor three orders of reflections independently.

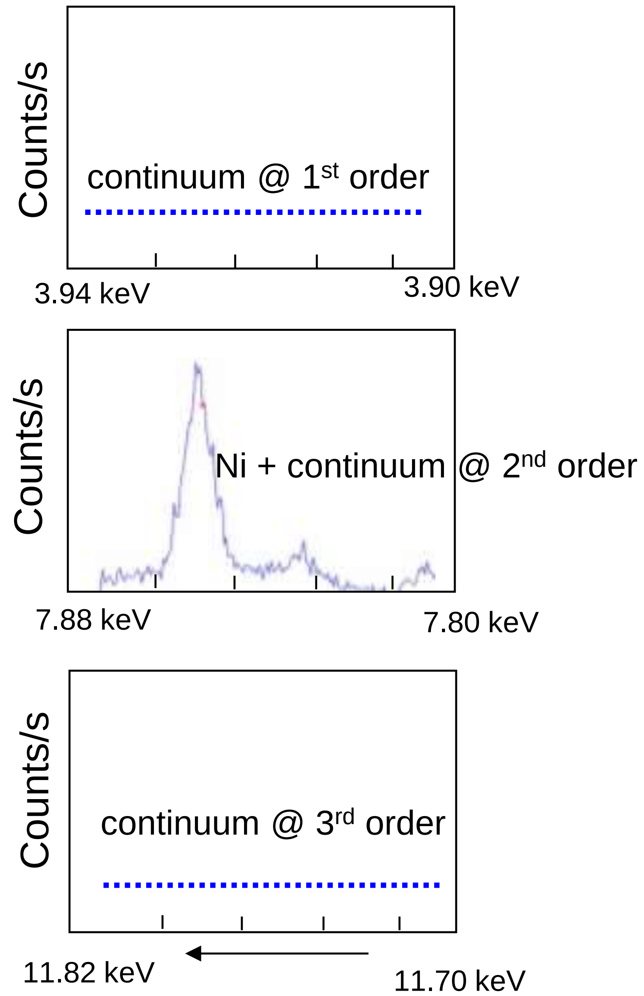

Development of novel gas detectors for soft X-ray

Lines to be measured:

Ni^{26+} [$1s^1 2p^1$]→ [$1s^2$], I(E)=1.59 Å (7.80 keV)

W^{46+} [$3p^5 3d^{10} 4d^1$]→ [$3p^6 3d^{10}$], I(E)=5.194 Å (2.39 keV)

X-ray detector(s) - functional requirements for JET

- Measure in parallel Ni^{26+}(7.8 keV) in second order and 3.9 keV in first order on one detector, and W^{46+}(2.4 keV) in first order on a second detector
- High quantum efficiency
- Ease of operation and maintenance
- Space resolution in x direction ~ limit 1.2 mm or smaller (0,8 mm)
- No spatial resolution in y direction
- ~200 independent channels
- Counting rate (limit) ~100 kHz- 1 MHz

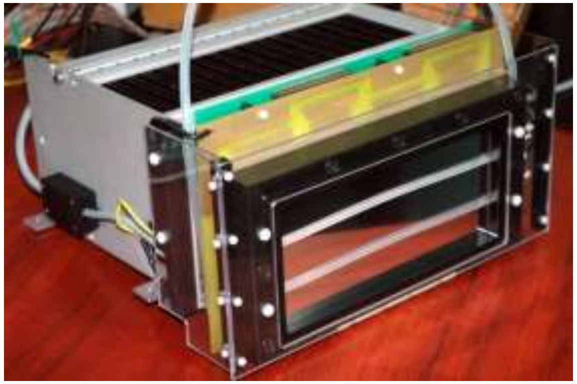

GEM for x-ray diagnostic

Advantages of the new generation GEM as detectors in high-resolution x-ray diagnostics:

The possibility to separate the amplification stage from the readout electrode, thus, the shape of the flat readout electrode closing the detector does not influence the amplification process.

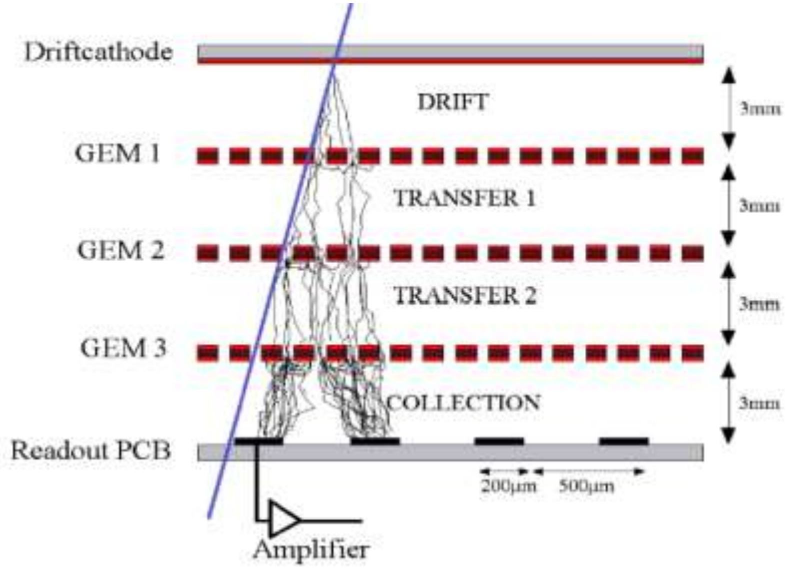

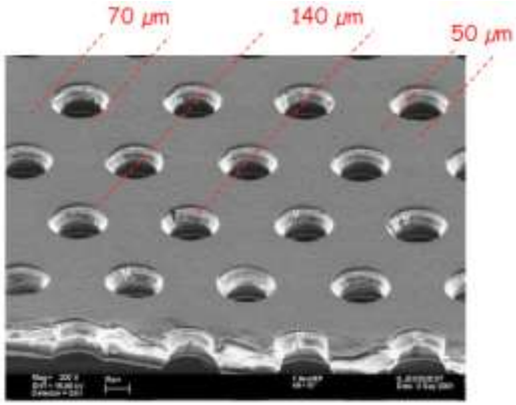

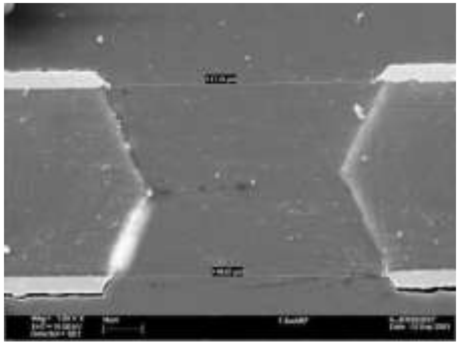

In consequence:

- High counting rate ~ 10^6 $mm^{-2}s^{-1}$
- Large gain range
- Good spatial resolution

Detection concept

- Gas detector (204x 90 mm^2)
- Detector operated in gas flow mode
- Construction materials: „all plastic" (delrin was chosen)
- High charge gain
- Stable operation at wide range of X-ray rates
- Good energy resolution

→ Triple GEM structure

- High detection efficiency → thin plastic metalized window
  → gas mixture

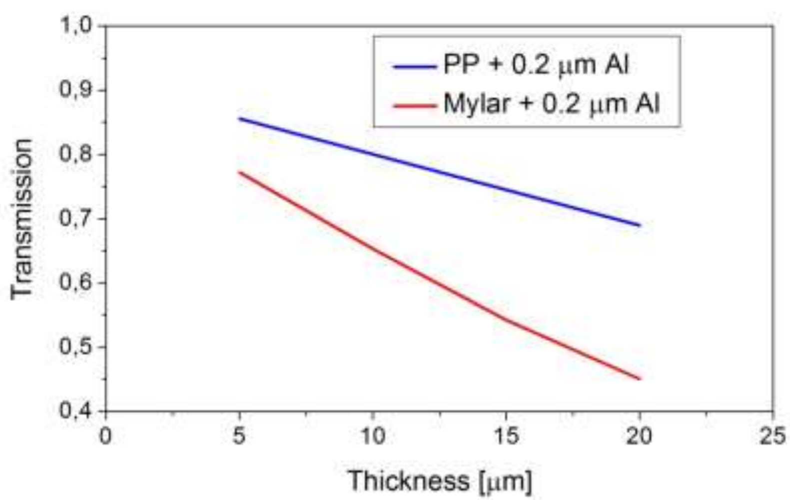

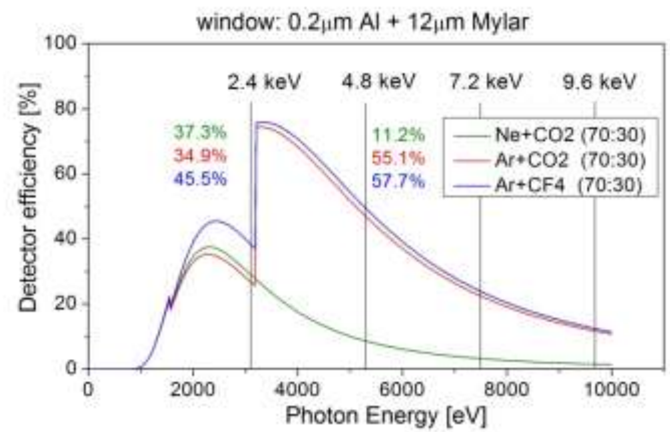

Detector structure

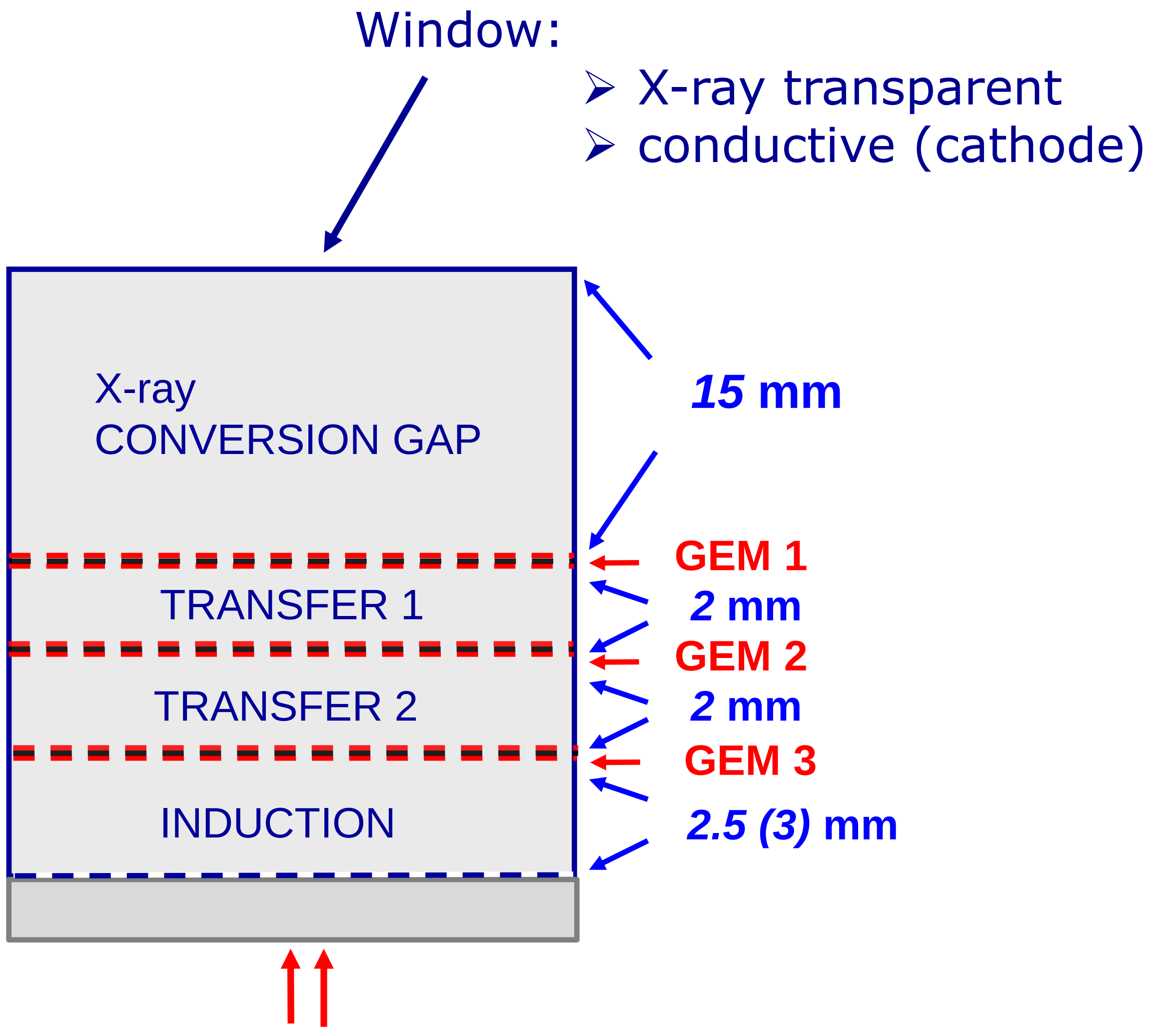

Readout plane with *0.8* mm strip pitch (*256* strips)

Detection module

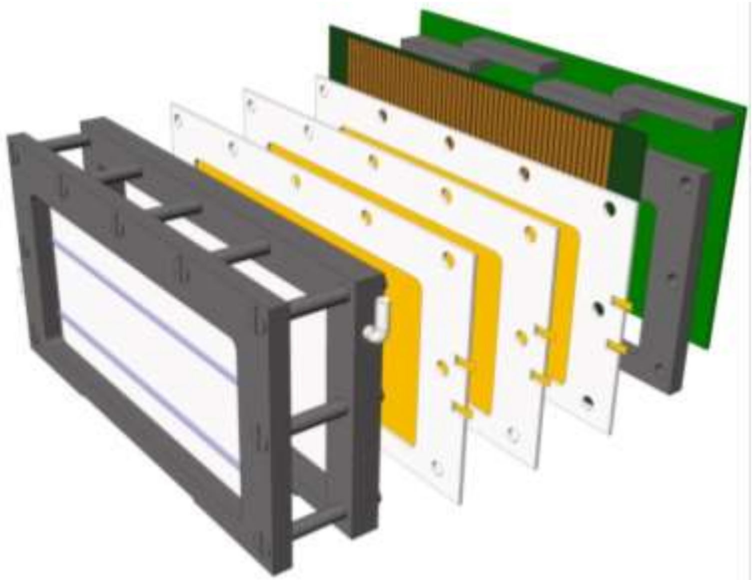

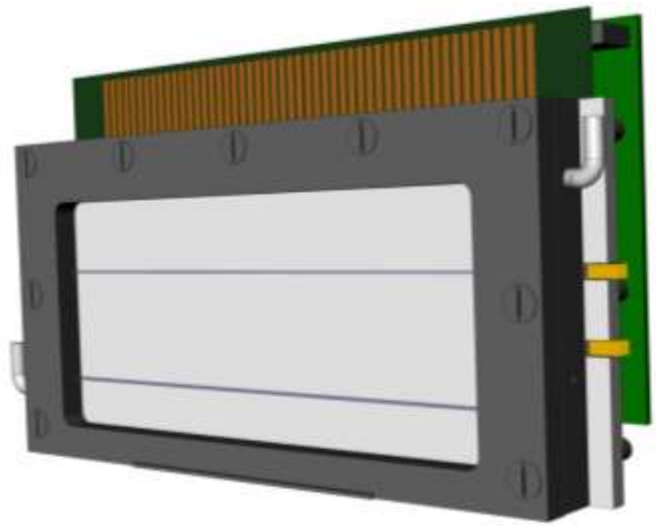

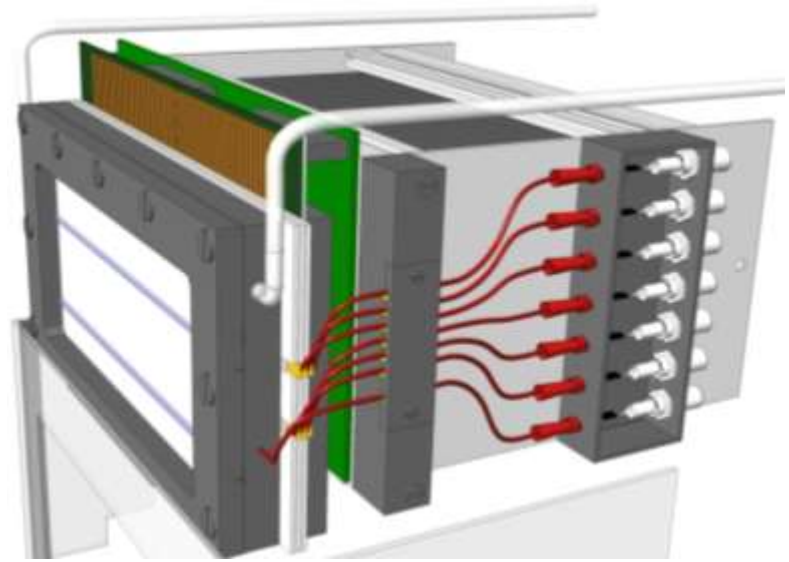

- Window: aluminized mylar: 12 μm (Ni) and 5 μm (W)
- Window plane = cathode with applied HV ~5kV
- Delrin frames
- Gas mixture : Ar + CO_2 (30%)
- Gas flow: 30 ml/min
- The read-out strip plane with 1.27 mm pitch and 0.05 mm gap between the edges

Detector readout

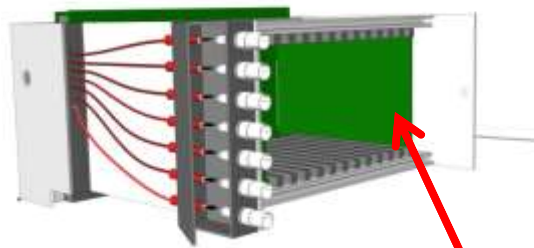

DETECTOR

256 channels

16 x 16 amplifiers & filters

ADC

FPGA

256

PC & Matlab

Laboratory tests

$^{55}Fe \xrightarrow{\text{electron capture}} {}^{55}Mn \rightarrow E_\gamma = 5.9\ \text{keV}$

Laboratory tests

^{55}Fe $\xrightarrow{\text{electron capture}}$ ^{55}Mn → $E_\gamma = 5.9$ keV

Position reconstruction based on center of gravity of strip signals

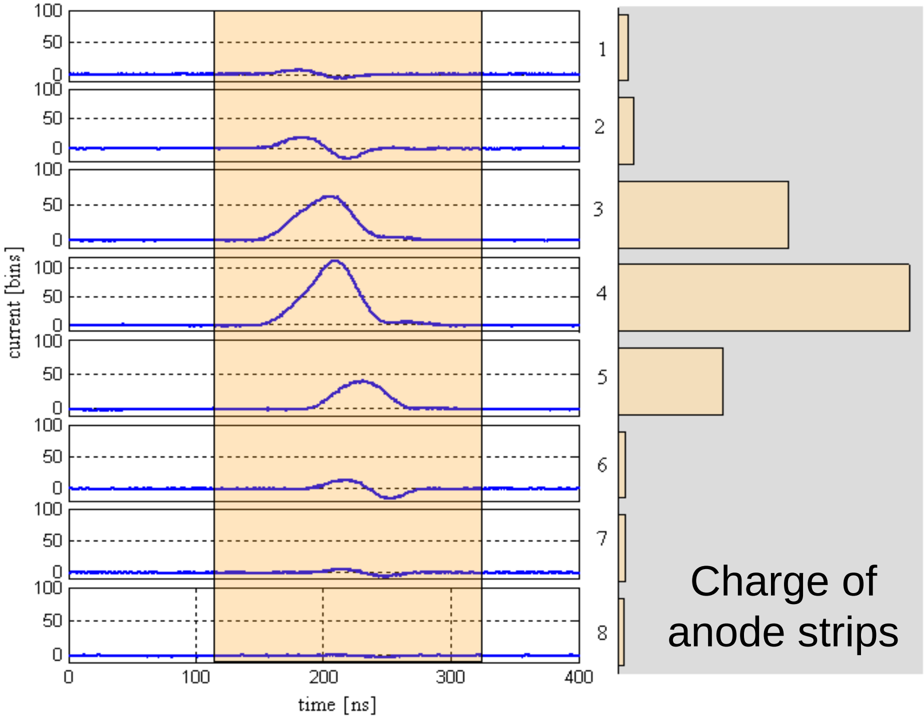

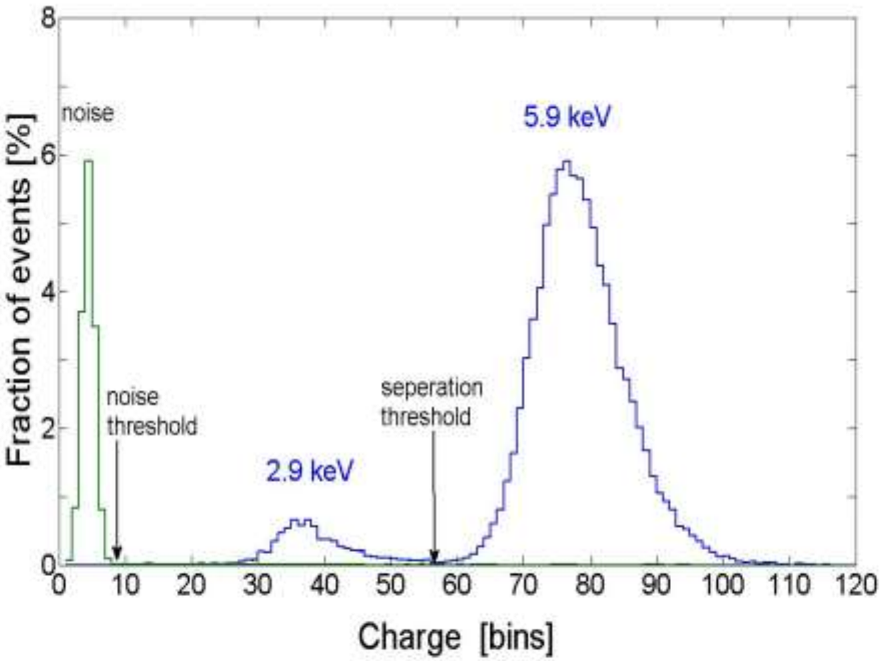

Energy := total cluster charge

Anode current signals for 8 strips (left) and corresponding relative charges (without offset compensation) (right) calculated within time of 200 ns (marked window)

New end-port window of KX1

„W” window
5 μm mylar

„Ni” window
12 μm mylar

Installation

Helium buffer in W detection module

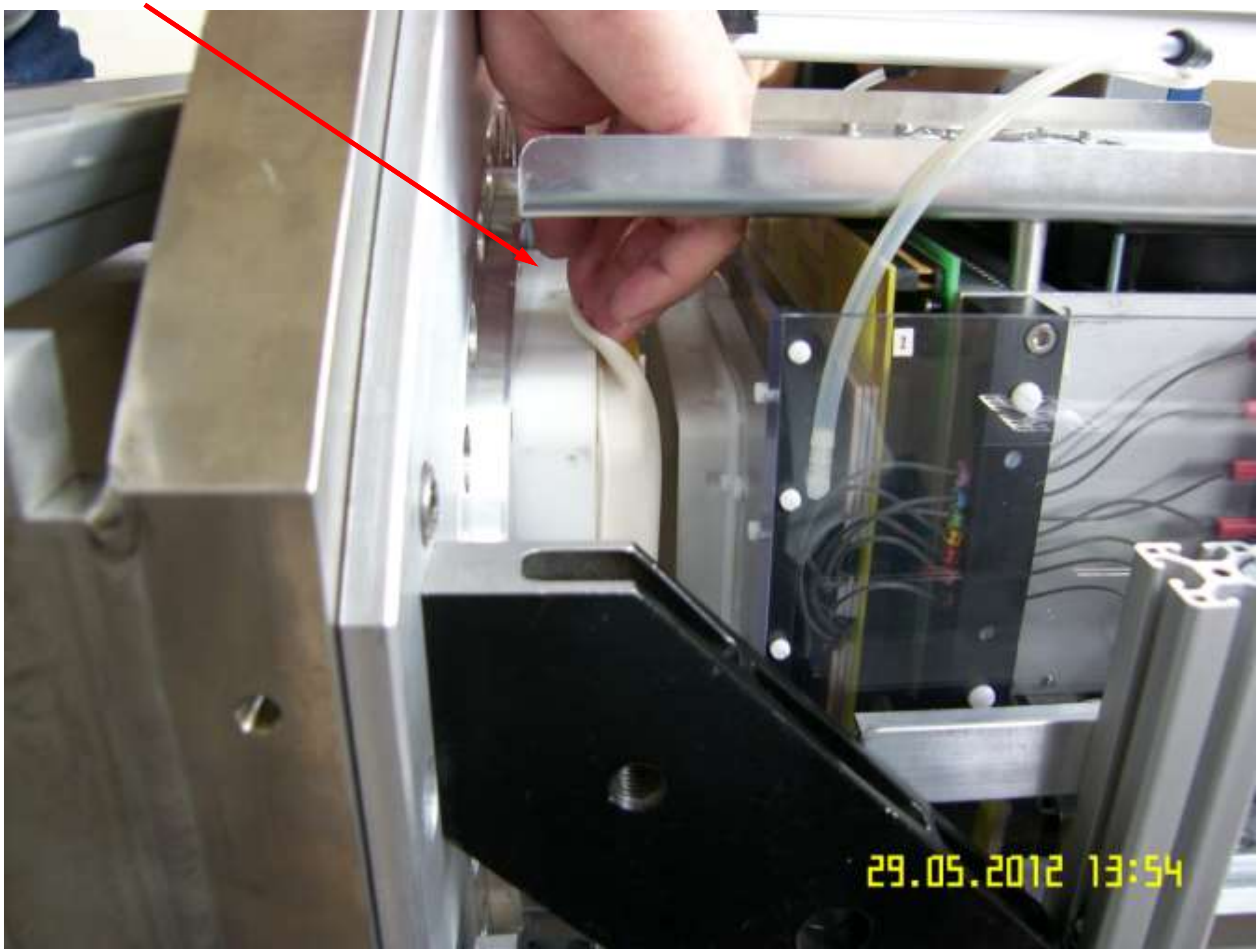

Installation

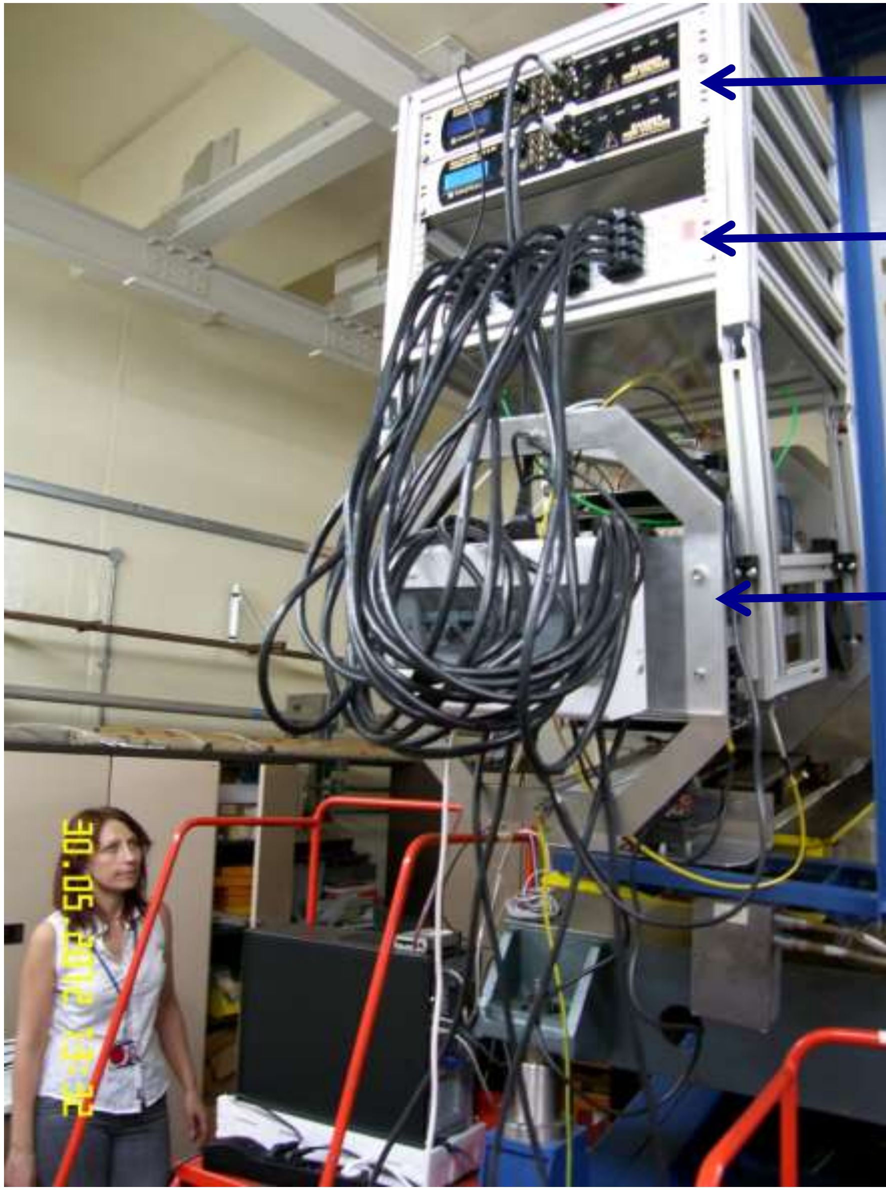

HV modules

FPGA electronics

Detection modules

Ni spectrum

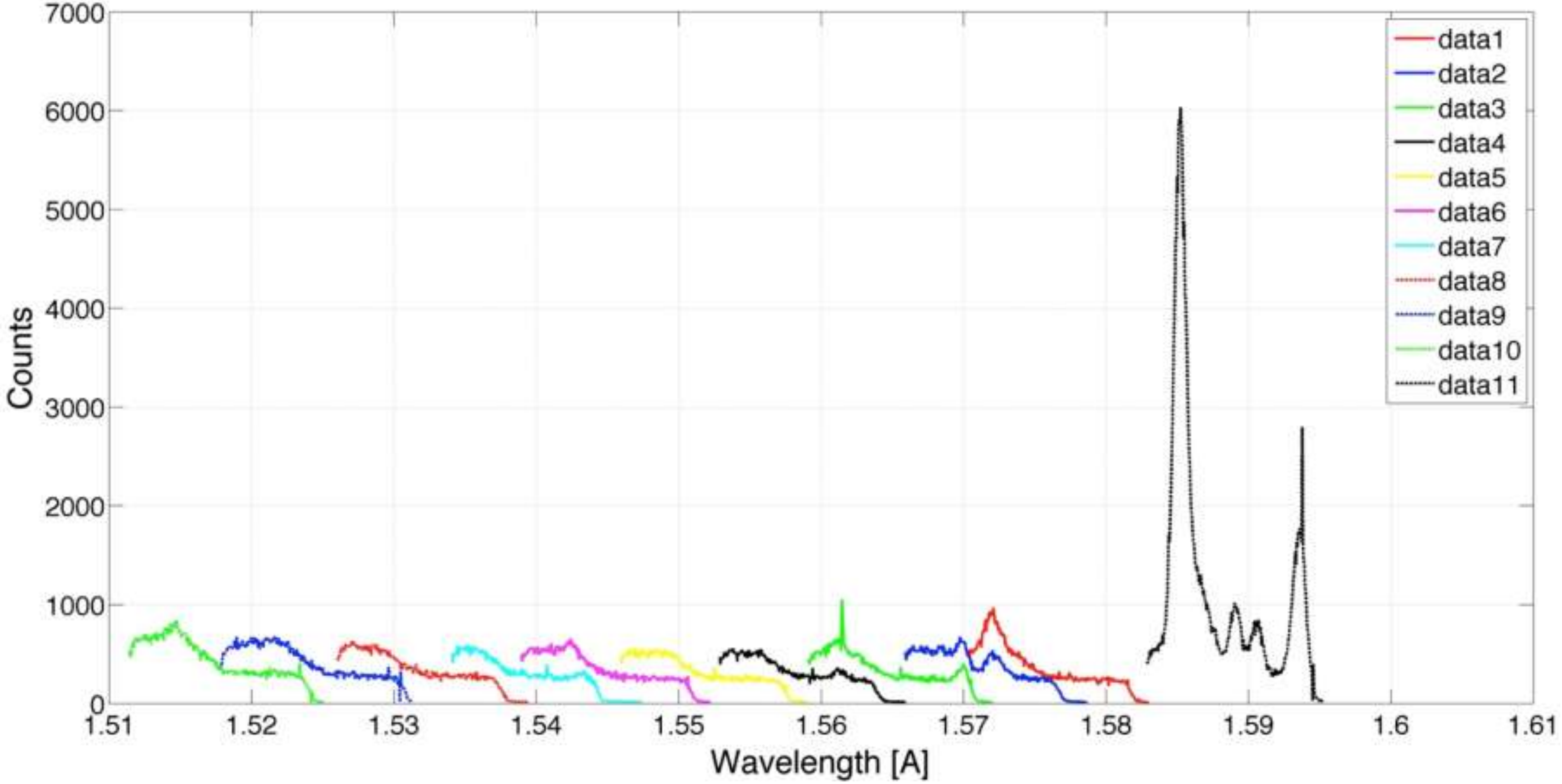
7000
6000
5000
4000
3000
2000
1000
0
Counts
1.51
1.52
1.53
1.54
1.55
1.56
1.57
1.58
1.59
1.6
1.61
Wavelength [A]
data1
data2
data3
data4
data5
data6
data7
data8
data9
data10
data11

Tests/First Measurements -Challenges

- clear dependence on p/T → correction in software
- broadening of Fe peak → proper voltage on each detector gap
- high temperature issue → lower frequency of data acquisition
- dependence of gain on rate/nonlinear regime of operations

  → optimal voltage divider (higher max. currrent),

  → increaseing of AFE amplification (operating in linear regime, better linearity)
- Signal non-continuity at FMC connections → correction in software

Status and plans

- ✓ detection area: x = 204 mm, y = 90 mm,
- ➢ rate capability 10^5 $mm^{-2}s^{-1}$, HV supply circuit should be optimized
- ✓ position resolution in direction perpendicular to the strips: pitch of strips smaller than ~1.27 mm,
- ✓ about 256 individual active channels shall be supplied per detector,
- ✓ significant improvement of QDE from ~8% level in previous KX1 set-up,
- ✓ high time-resolution ~ 10 ms, long term verification of the stability, optimization of the firmware, new carrier back-plane
- ➢ read-out of two (or three) spectral orders, energy tagged diffraction patterns to be implemented
- ✓ high line to continuum ratio,
- ✓ high stability of the efficiency (~5% independent of changes in atmospheric pressure, for count rates up to 2 MHz),
- ➢ energy resolution ~20%, working point of the chambers should be optimized, calibration procedure should be developed and implemented in the firmware
- ✓ good detection conditions for measurements of W impurity level, energy distributions should be studied and understood

Neutron yield monitor as an indicator of fast particles confinement

B. Bienkowska, R. Prokopowicz, M. Scholz
IPPLM – EURATOM Association

Background

- DT/DD neutron ratio as an indicator of tritons confinement in deuterium plasma
- d+d → p+**t**   d+t → n+**α**
- DD tritons ↔ DT alphas

similar slowing-down, diffusion, confinement properties

Method

- Neutron detection by beta-particles recording
- Simultaneous measuring of 2.5 and 14 MeV neutron detection by gaseous detectors
- Selected nuclear reactions

$n_{(2.5\ \text{MeV})} + {}^{9}Be \rightarrow \alpha_{(1.0\ \text{MeV})} + {}^{6}He_{(T_{1/2}=0.8\ \text{s})} \rightarrow {}^{6}Li + \beta^{-}_{(1.5\ \text{MeV})}$

$n_{(14\ \text{MeV})} + {}^{20}Ne \rightarrow p_{(6.5\ \text{MeV})} + {}^{20}F_{(T_{1/2}=11\ \text{s})} \rightarrow {}^{20}Ne + \beta^{-}_{(2.5\ \text{MeV})}$

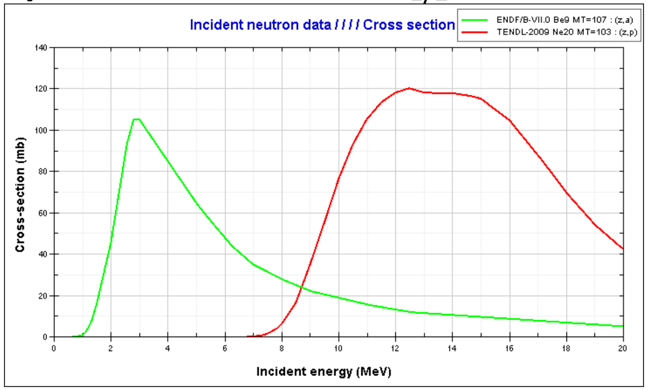

Measurements

- Construction, calibration and operation of the 2.5 MeV neutron detector (demonstration of the method)

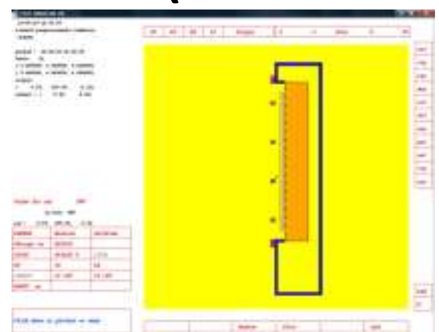

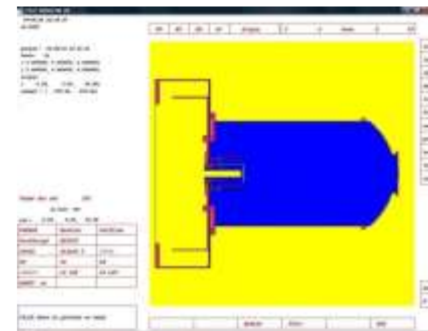

- Construction and preliminary tests of prototype GEM detector (β particles)

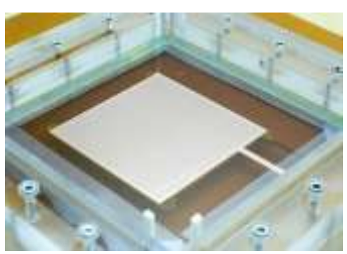

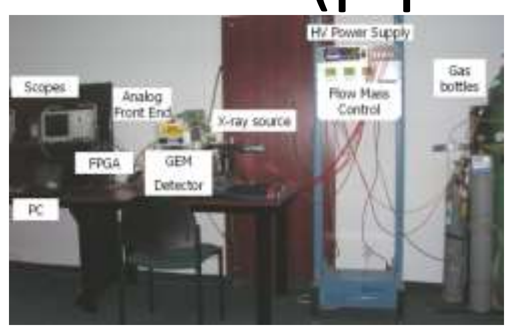

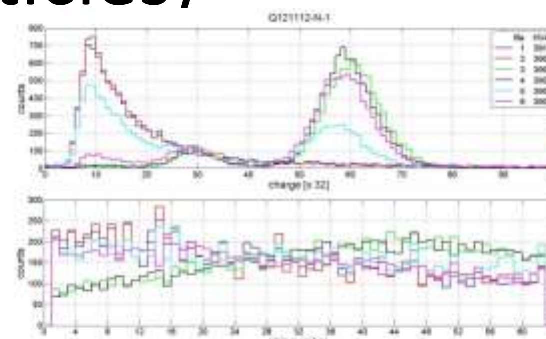

Plans

to be done

- further GEM tests
- adapt GEM detector for neutron measuring

CVD diamond detectors for measurements of fusion plasma products

K.Drozdowicz, J.Dankowski, B.Gabańska,
A.Igielski, A.Kurowski, B.Marczewska, T.Nowak,
M. Scholz, U.Woźnicka
and M.Jaskóła, A.Korman (NCBJ)

Institute of Nuclear Physics of the Polish Academy of Sciences, Kraków
NCBJ Swierk/Otwock, Poland

Semiconductor detector

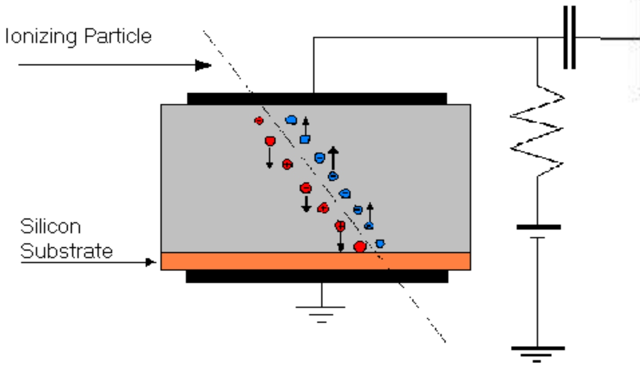

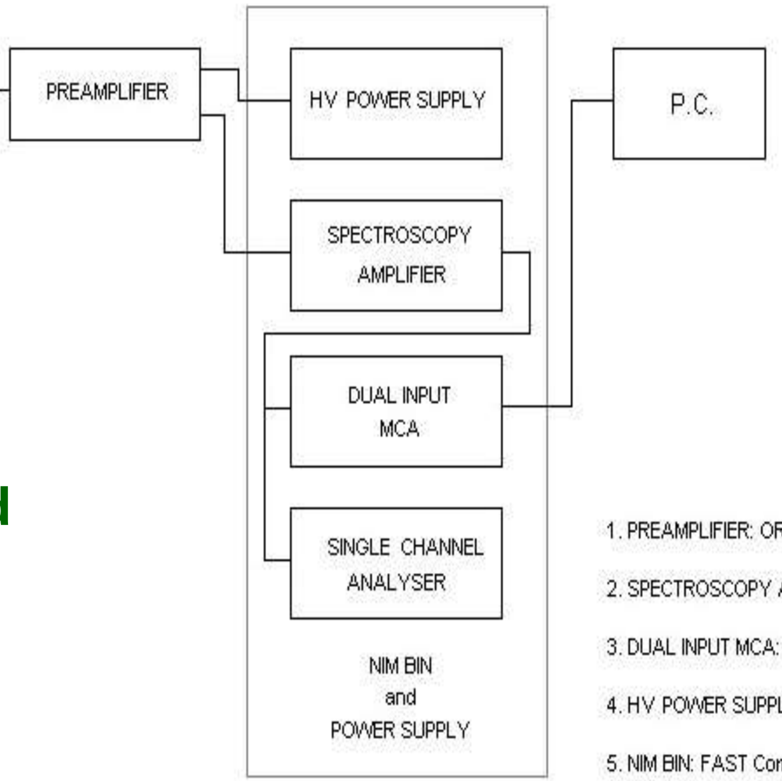

1. PREAMPLIFIER: ORTEC 142A
2. SPECTROSCOPY AMPLIFIER: ORTEC 672A
3. DUAL INPUT MCA: ORTEC 550A
4. HV POWER SUPPLY: FAST ComTec NHQ 202M
5. NIM BIN: FAST ComTec 7032

e.g. Ge, Si, diamond

Diamond Detectors Ltd

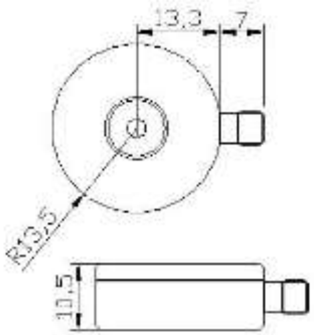

CVD monocrystal

2.5 mm x 2.5 mm x 50 µm

High purity**:** **Ni, B** < 5 ppb

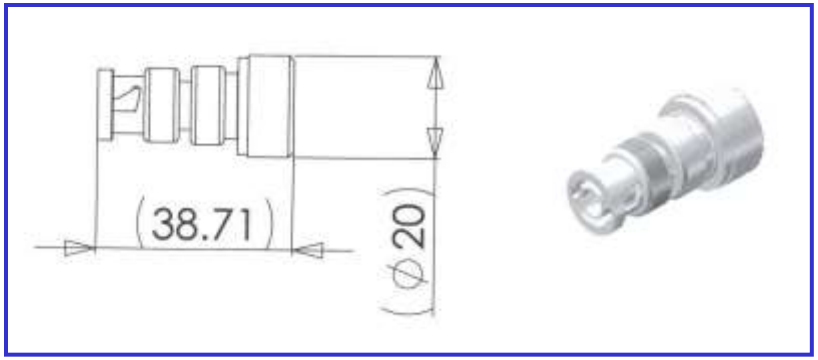

Advantages / Disadvantages of the diamond detector

- **Low noise**
- **Higher temperature of work**
- **Radiation hardness**
- **Chemical inertness**
- **Mechanical robust**

- **Smaller signal (< ½ signal from Si)**
- **Relatively new material → a few manufacturers**
- **Higher cost**

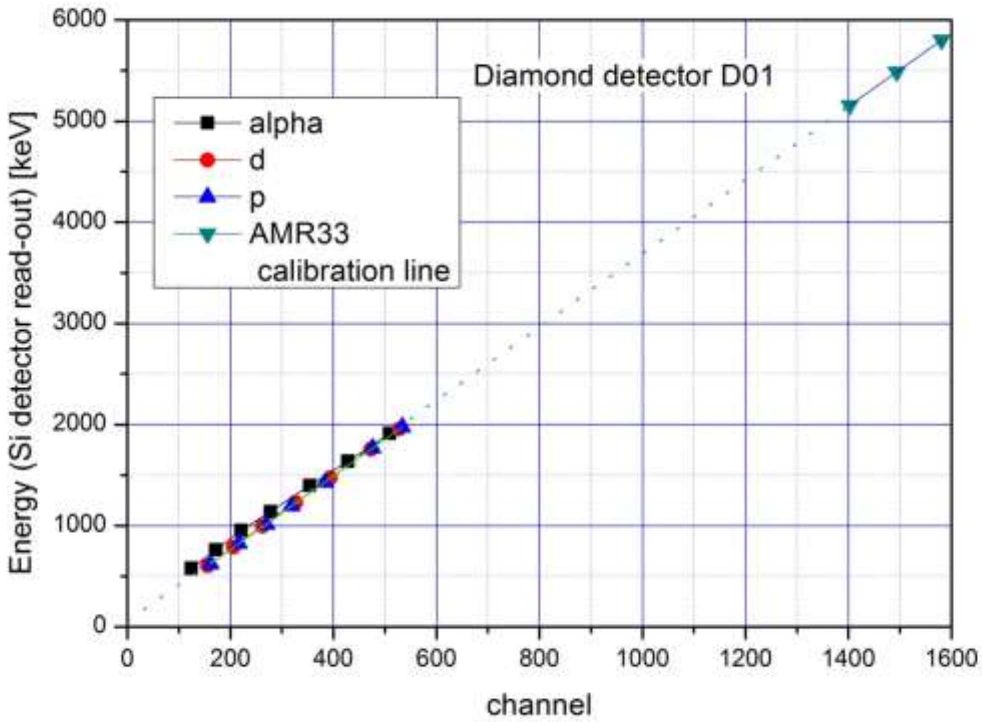

Response of the diamond detector D01
for the α calibration source (AMR33, triple energy)
and mono-energetic ions (α, *d*, *p*).

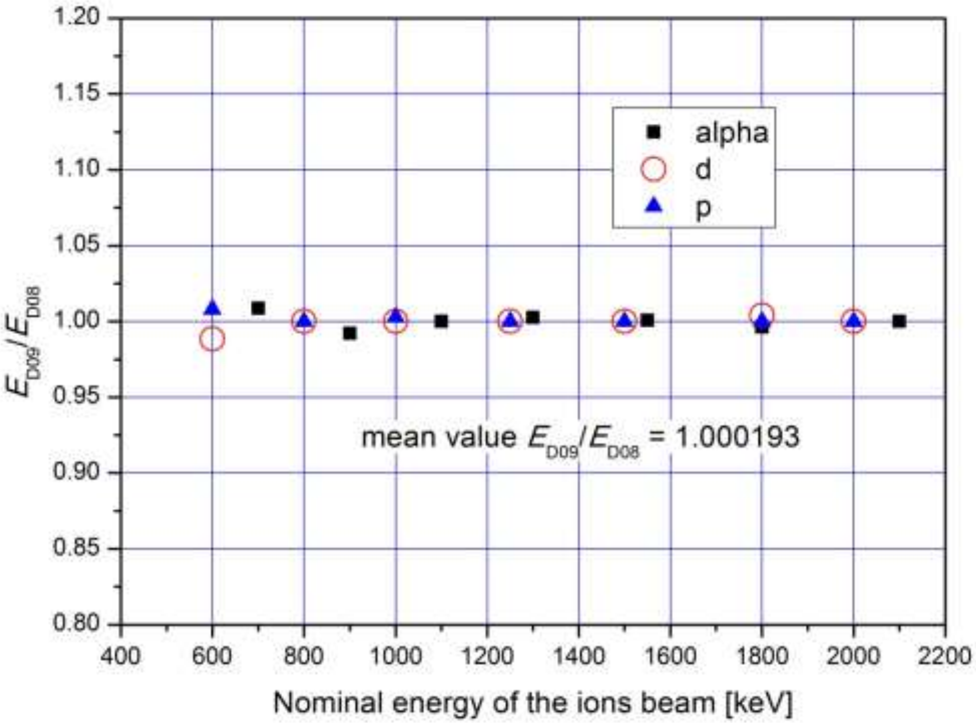

Comparison of detectors D08 and D09.

The CVD diamond detector in a mixed radiation field.

Response of the CVD diamond detector for spectrometric measurement of fast ions in a mixed radiation field was tested in the experiments at the 14 MeV neutron generator.

The fast neutron generator at the Institute of Nuclear Physics of the Polish Academy of Sciences in Kraków (Poland) is a linear accelerator where the deuteron incident beam induces the nuclear reaction d(t,n)α in a tritium target. The energy of alpha particles produced here in the D-T reaction is the same as the energy of alpha particles created in the hot plasma in tokamak (maximum energy 3.5 MeV).

Other reactions in the target also occur and the energetic spectra from three main nuclear reactions:

$$^{3}T(d,n)^{4}He, \quad ^{2}H(d,p)^{3}H \quad \text{and} \quad ^{3}He(d,p)^{4}He$$

at a high flux of deuterons were measured.

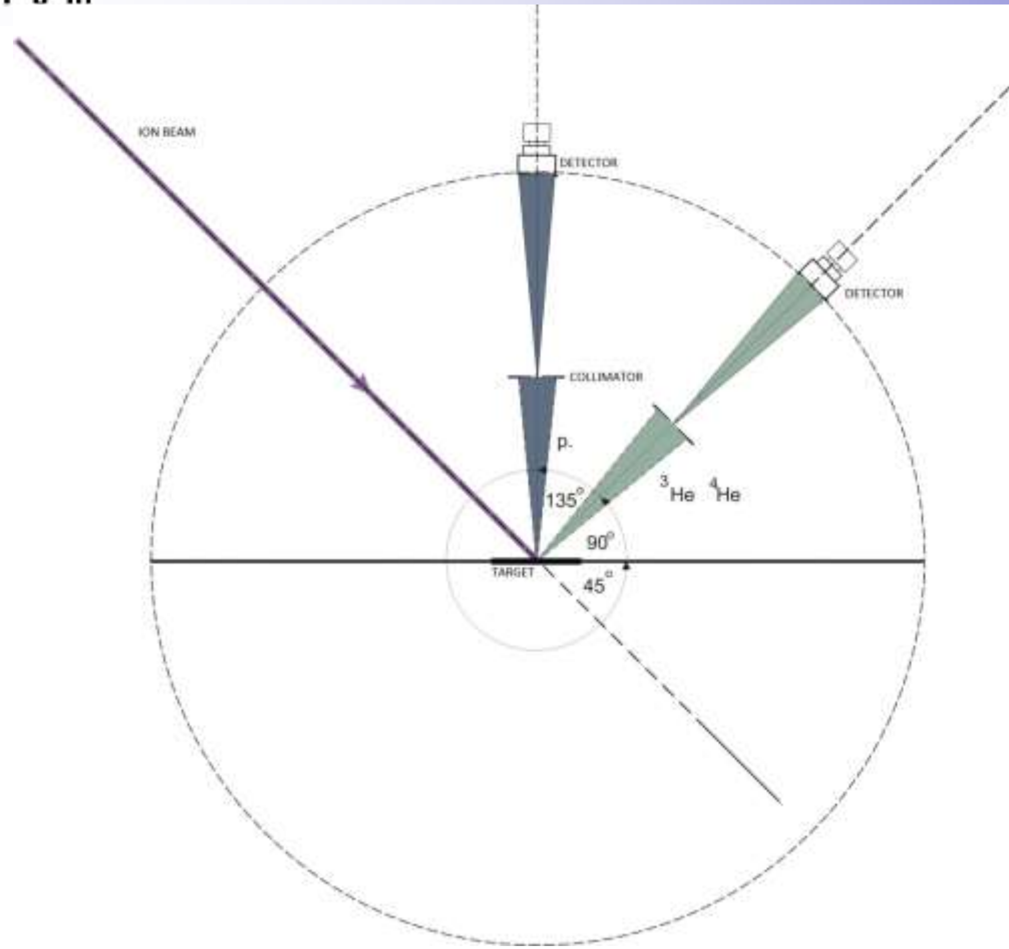

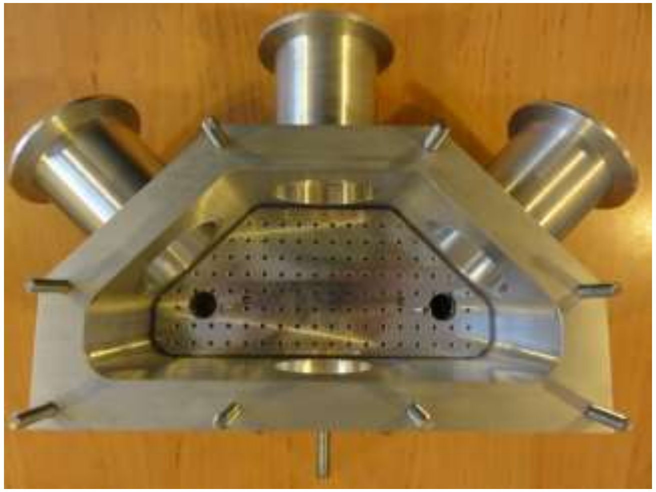

Idea and a view of the measuring chamber built for experiments with diamond detectors in the mixed radiation field at the fast neutron generator in IFJ PAN [D-T, D-D, and accompanying reactions]

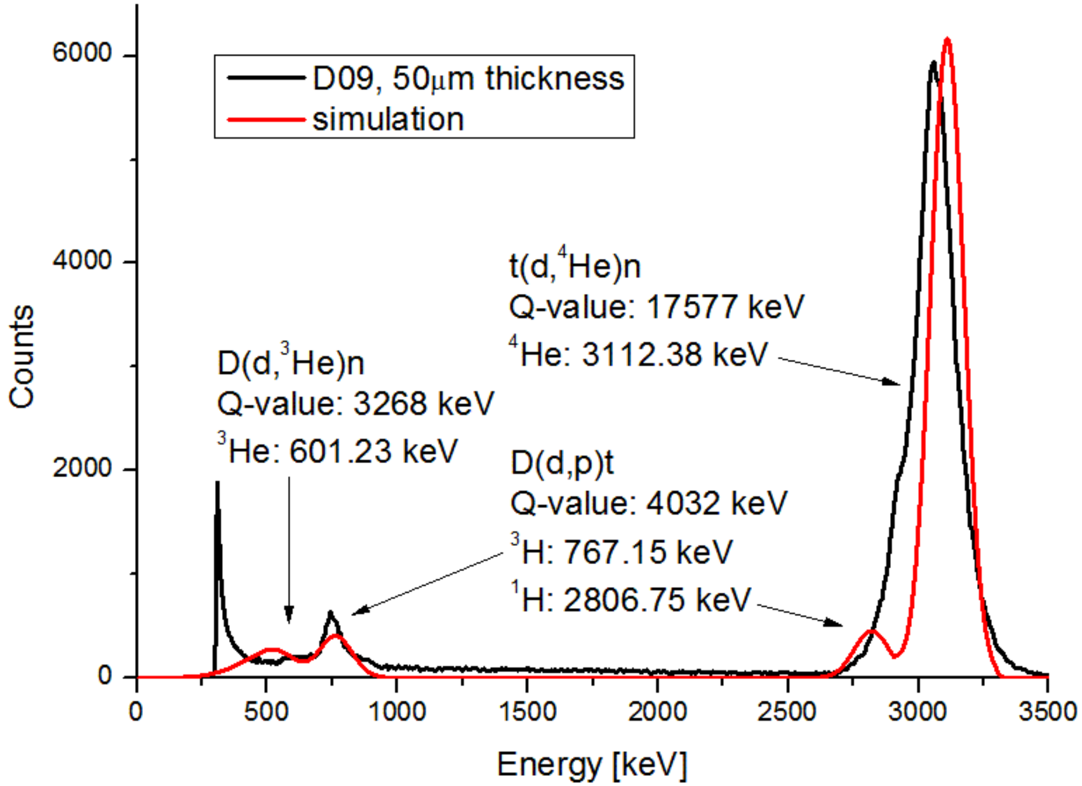

Example of the spectrum of alpha particles, protons, tritons, and He-3 ions, obtained by 50 μm thick diamond detector (D09) inside the vacuum measuring chamber at the 14 MeV neutron generator.

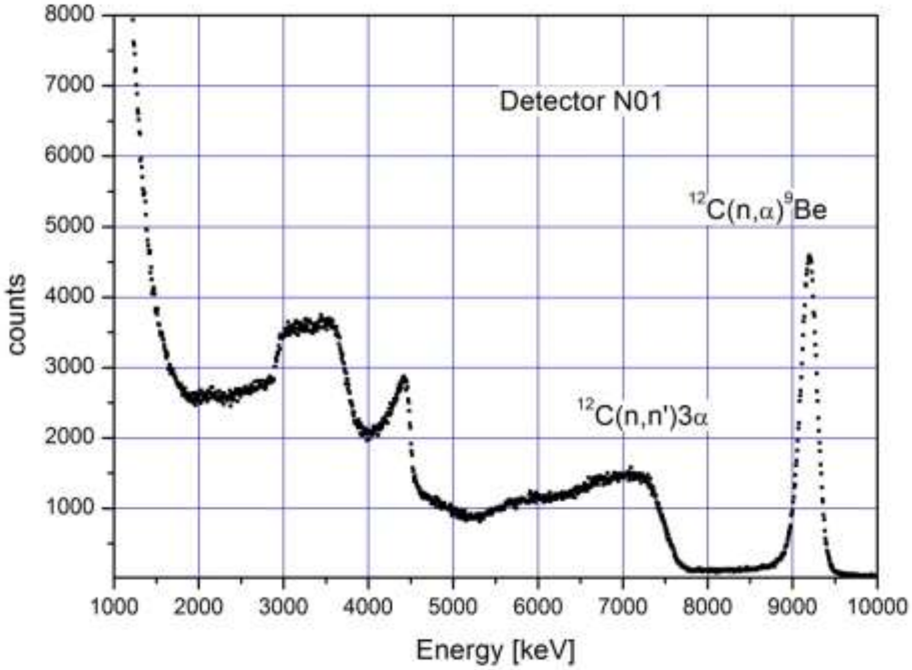

Fig. 23. Example of a response of the 500 μm thick diamond detector (N01) at the 14 MeV neutron generator (**neutrons** outside the measuring chamber).

Study of $LaBr_3$:Ce, $CeBr_3$ and NaI(Tl) Scintillators for Gamma Camera for Plasma Diagnostic in Tokamaks

P. Sibczyński, A. Gójska, M V.G. Kiptily, M. Moszyński,
J. Rzadkiewicz, M. Scholz, A.E. Shevelev, A. Syntfeld-Każuch,
Ł. Świderski, M. Tardocchi, I. Zychor

NCBJ, IFJ PAN, JET, ENEA

Motivation

- Gamma ray spectroscopy is a powerful diagnostic that can be used for studying fast ions behavior in tokamak plasma.
- Gamma ray spectra provide information on the spatial and energy distribution of fast electrons and ions.
- This knowledge is of a crucial importance for future thermonuclear reactor development.

ITER tomography system

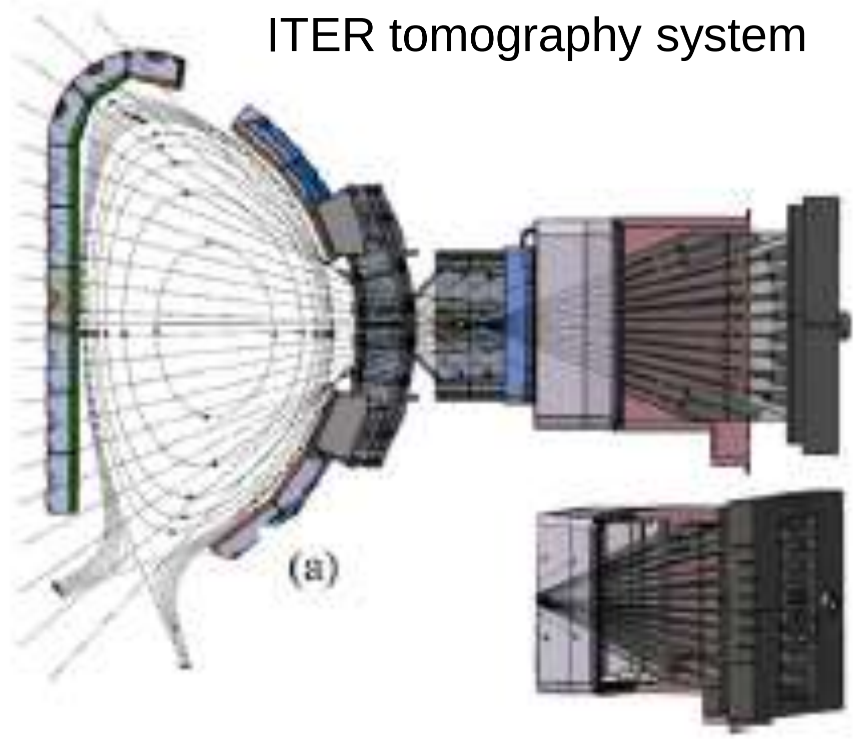

Research program

- Many scintillation materials were considered for gamma ray monitoring in tokamaks. While NaI(Tl), CsI(Tl) and BGO scintillators operate with high efficiency and energy resolution, they are characterized by a relatively long scintillation decay time.
- For this reason their use at high counting rate measurements required for diagnostics of fusion plasmas in tokamaks is not possible.
- Thus, our aim is to compare the properties of the 'slow' CsI(Tl) and NaI(Tl) crystals with 'fast' crystals (e.g. $LaBr_3$:Ce) as potential scintillators for gamma ray camera.

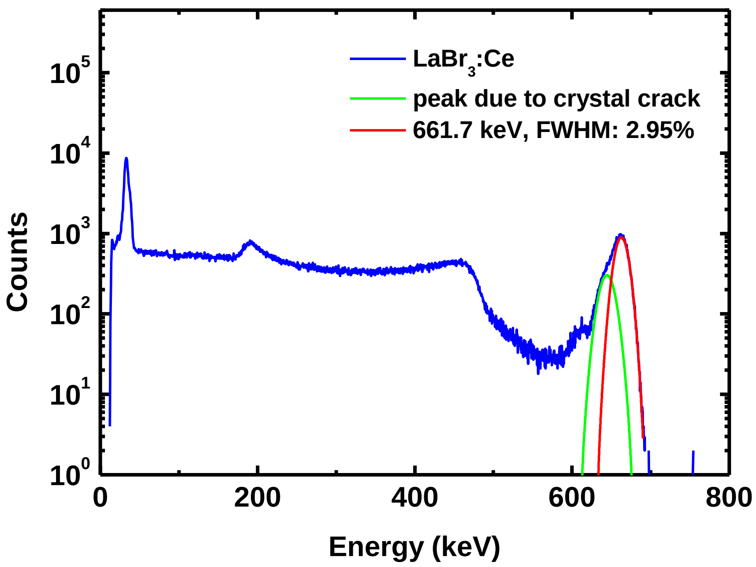

Preliminary results

- The $LaBr_3$ crystal tested in our project shows very good energy resolution, which is about 2.95 $\pm$ 0.03 %.
- It is comparable to that presented in other paper [1].

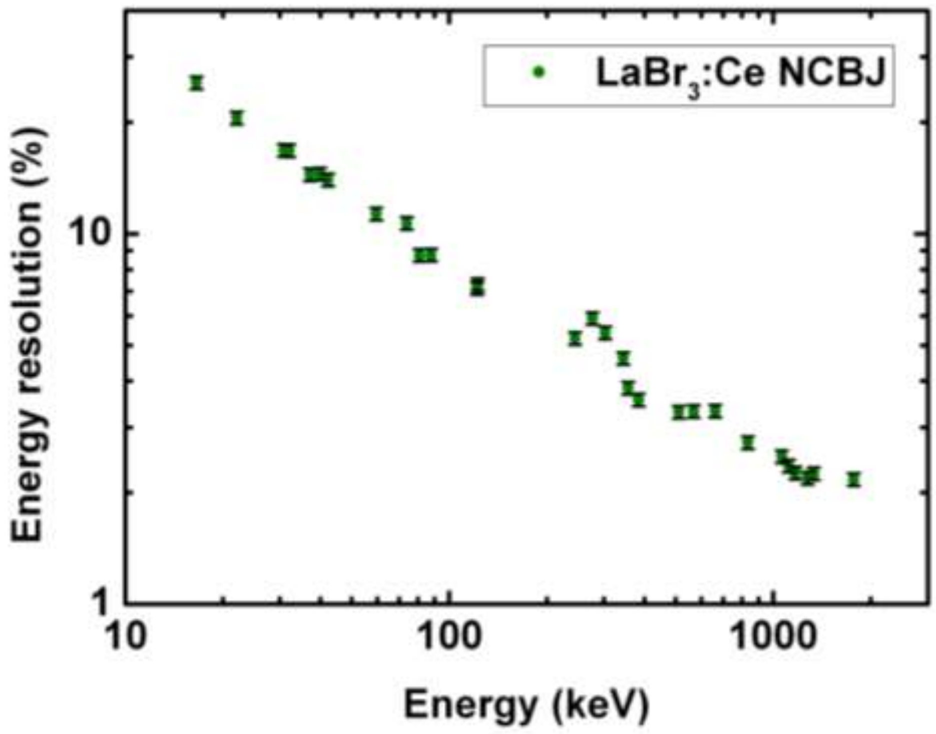

[1] M. Moszynski et al. *IEEE Transactions on Nuclear Science, vol. 55.*

Preliminary results

The $LaBr_3$ shows nearly proportional response to gamma rays – above 100 keV the light yield generated by scintillator

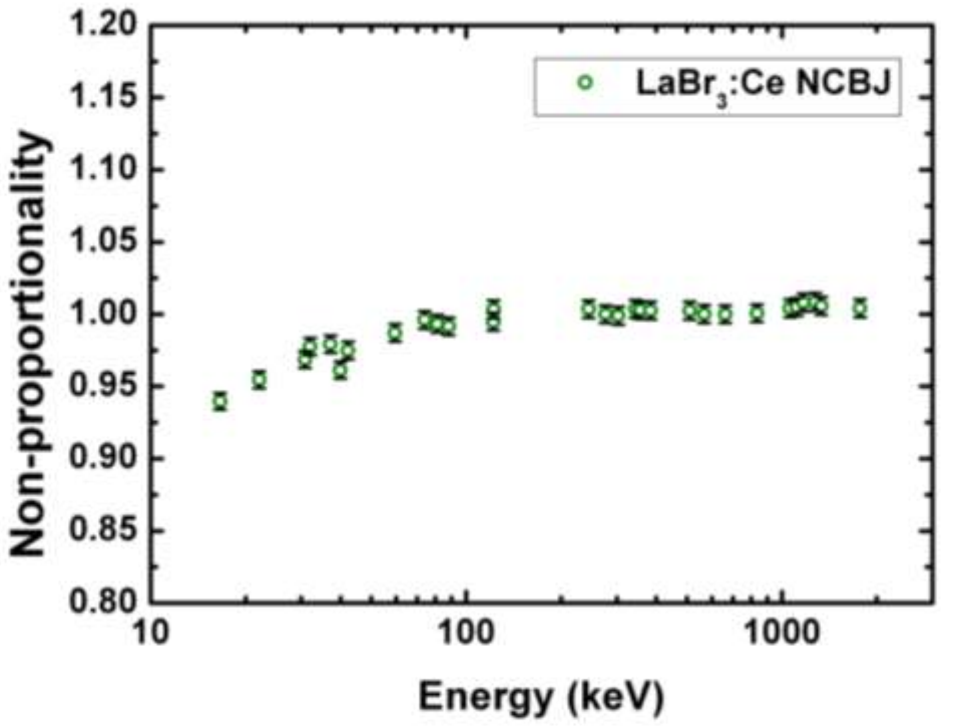

Plans for 2013

- **Testing other scitillator crystals**
- **Develope aqusition system based on the TUKAN solution (NCBJ product)**

Gateable MCP based Camera for VUV and Soft X-ray Imaging of Magnetically Confined Plasma

M. Paduch, J. Rzadkiewicz, M. Scholz, K. Tomaszewski, E. Zielinska

Institute of Plasma Physics and Laser Microfusion, Warsaw,
ACS Laboratory Ltd., Warsaw
Institute of Nuclear Physics of the Polish Academy of Sciences, Kraków

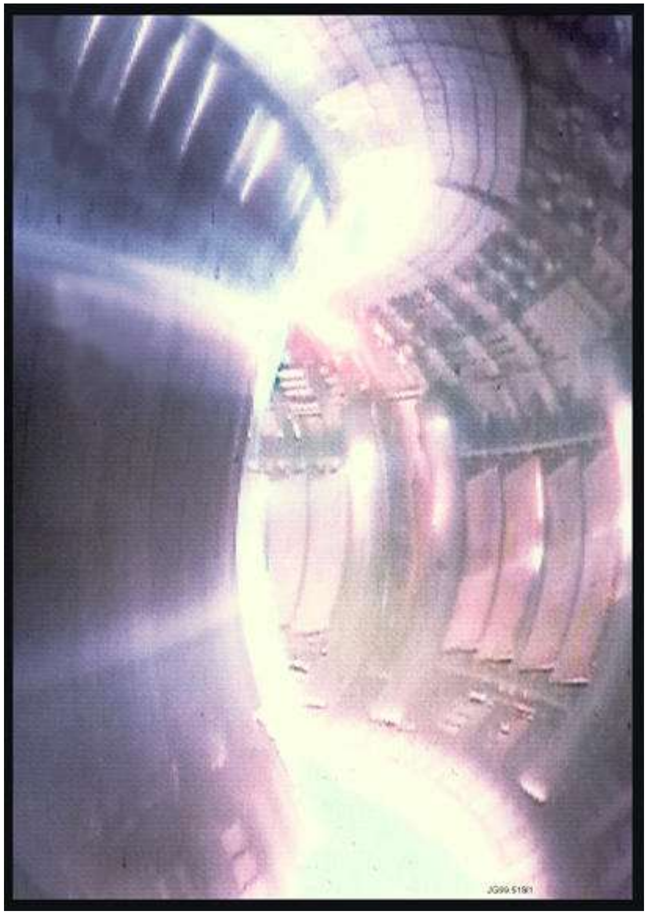

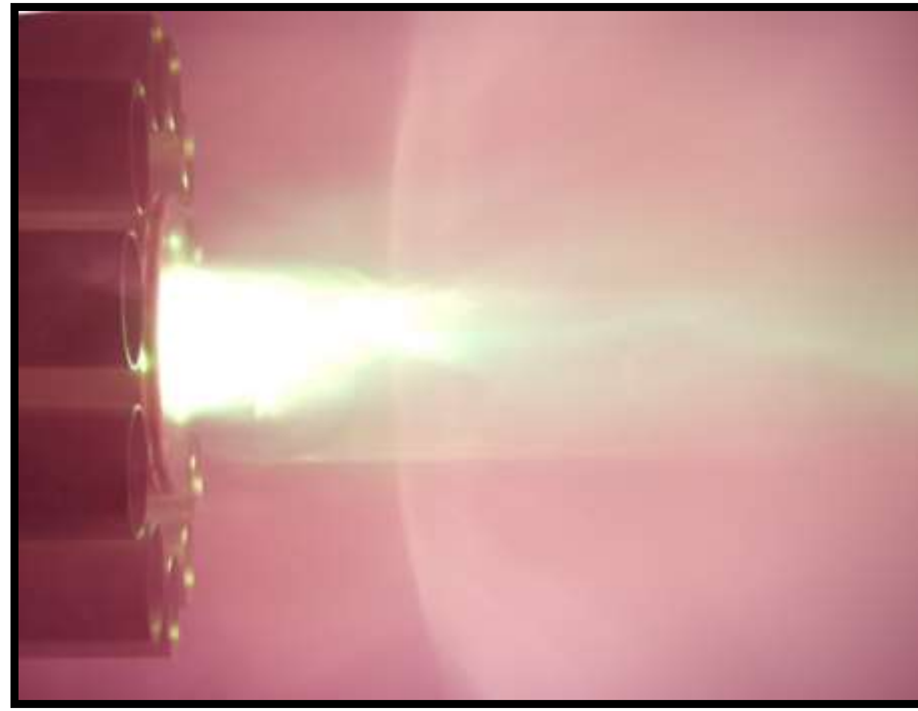

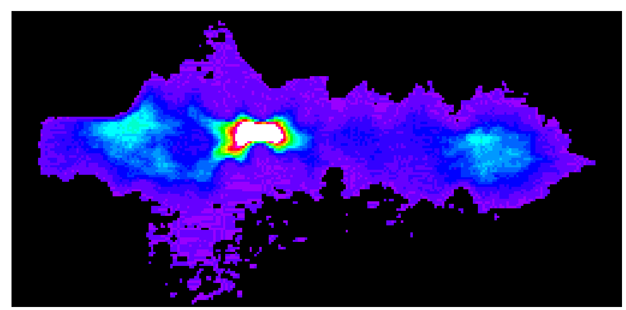

Basic Principle

Gateable Open MCP-based device play the role of primary image detector, radiation amplifier and fast or ultra-fast shutter

whereas CCD or CMOS (High Speed Video - HSV) cameras are applied only as final image detectors, allowing the storage (in digital form) of the images of the investigated object appearing on luminescent screens of gated primary image detector

General Layout:

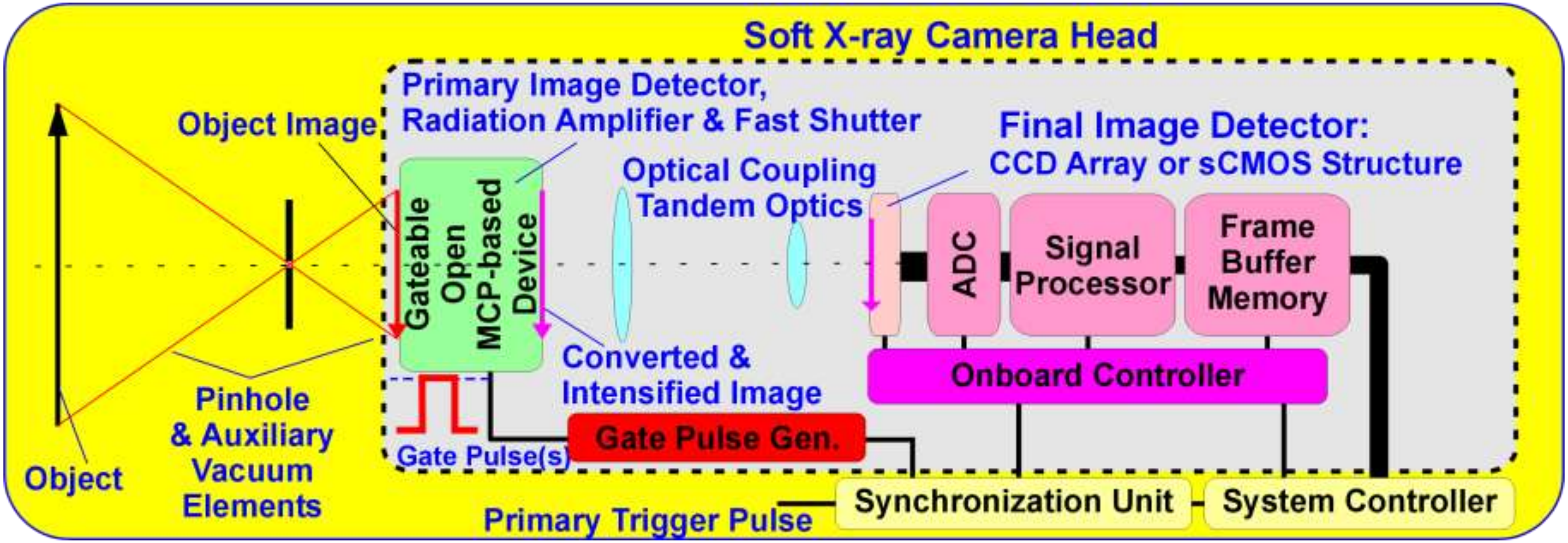

Microchannel Plate - MCP

A MCP is a secondary electron multiplier consisting of an array of millions of very thin glass channels (glass pipes, typically 6 –10 μm diameters) bundled in parallel and sliced in the form of a disk

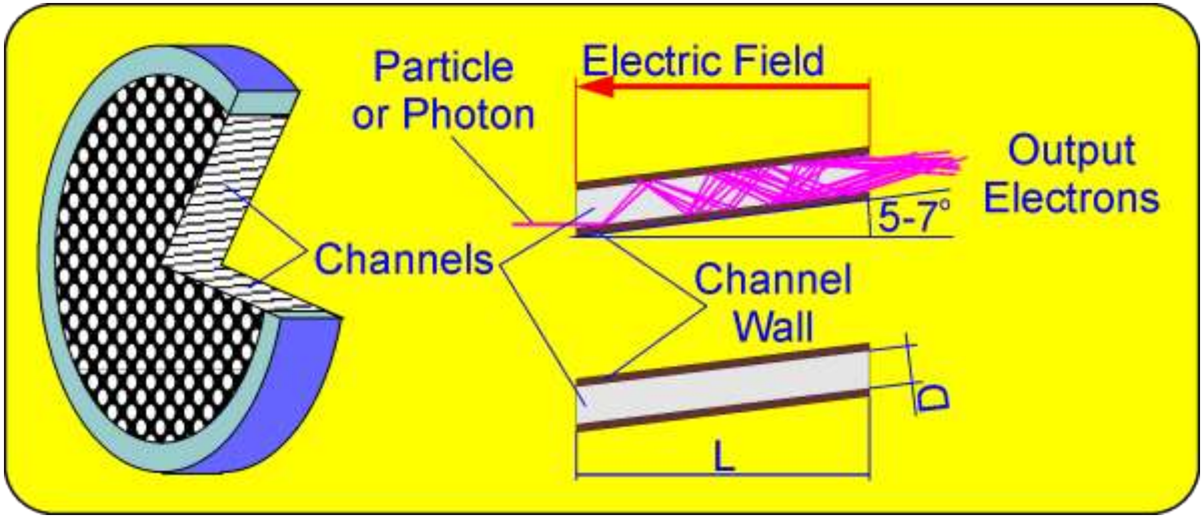

Each channel works as an independent electron multiplier - when a photon or particle enters a channel and hits the inner wall, secondary electrons are produced

This process is repeated many times along the channel wall and as a result, a great number of electrons (multiplication factors of up to four orders of magnitude) are output from the MCP

Principle of Operation

Principle of Operation

	Energy / Wavelength	Efficiency
Electrons	100 eV ... 500 eV	10 % ... 50 %
	500 eV ... 4 keV	50 % ... 75 % ... 50 %
	4 keV ... 100 keV	50 % ... 10 %
Ions	500 eV ... 3 keV	5 % ... 40 %
	3 keV ... 10 keV	40 % ... 70 %
	10 keV ... 50 keV	70 % ... 80 % ... 70 %
	50 keV ... 200 keV	70 % ... 40 %
Soft X-ray / UV-Radiation	0.2 nm ... 30 nm	3 % ... 16 %
	30 nm ... 115 nm	16 % ... 8 %
	115 nm ... 150 nm	8 % ... 2 %

Source - PROXITRONIC

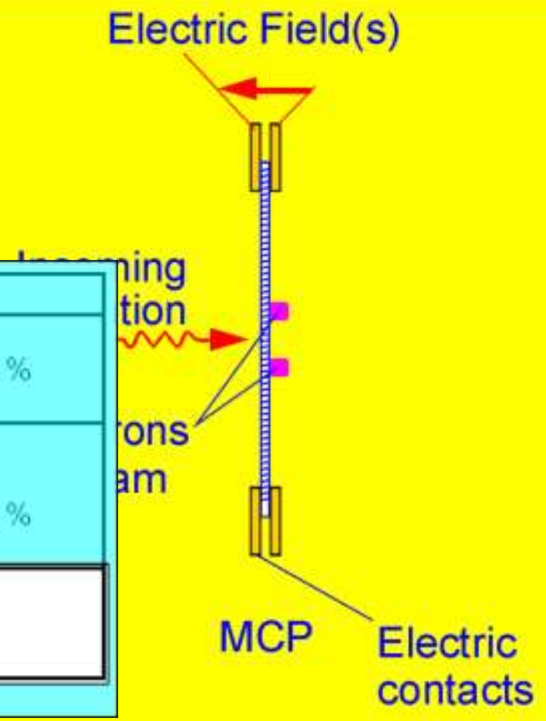

Principle of Operation

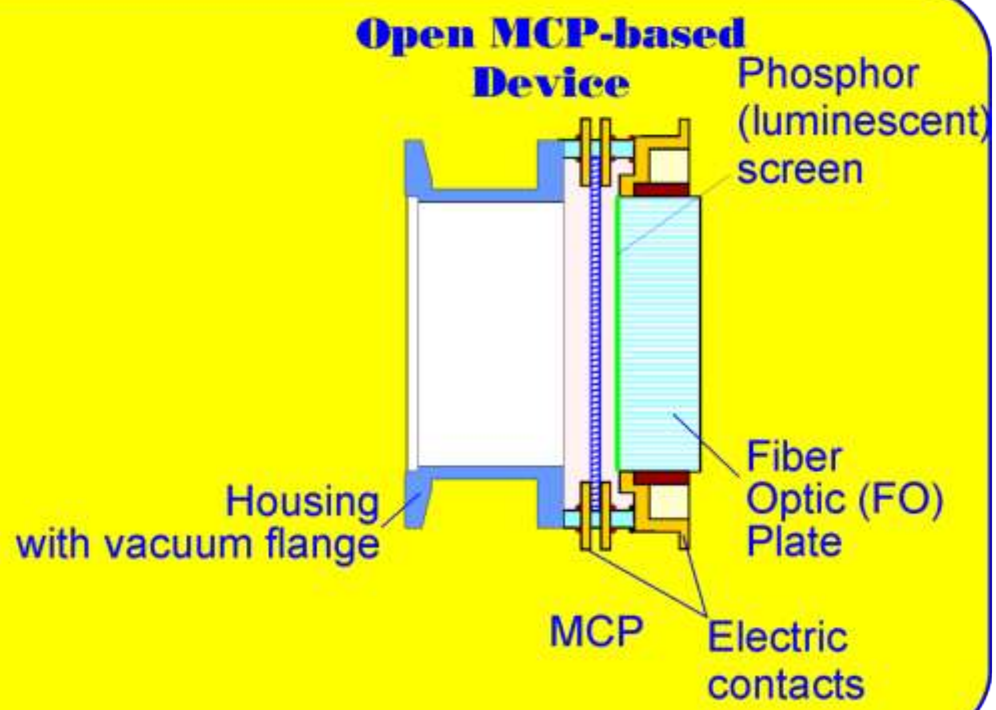

In order to convert electron stream into light, a phosphor screen should be added

MCP and a phosphor screen must be firmly assembled inside ceramic housing, which is durably combined with a vacuum flange
Such design is usually called – Open MCP-based Device

Principle of Operation

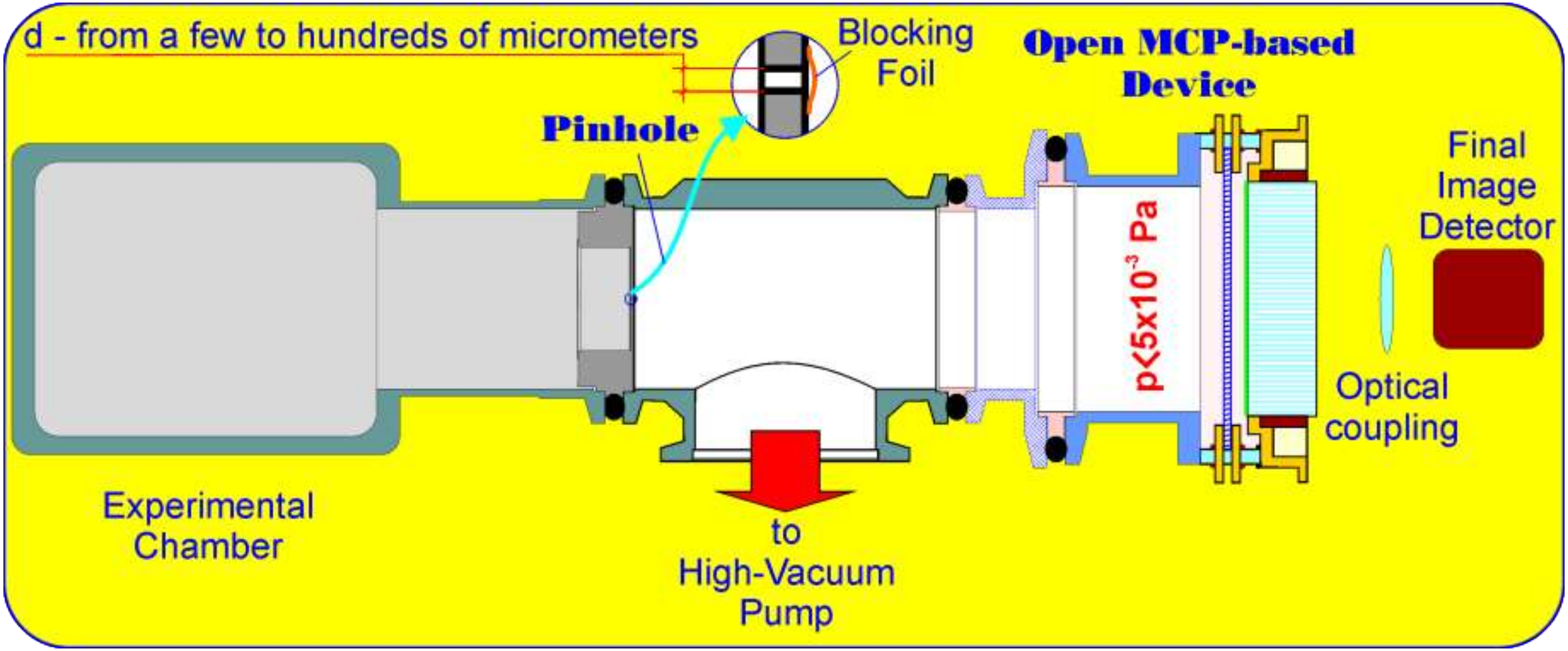

In order to prevent gas leakage from experimental chamber
a pinhole has to be?
covered by blocking foil

Different Arrangements of Open MCP-based Devices

Standard Design

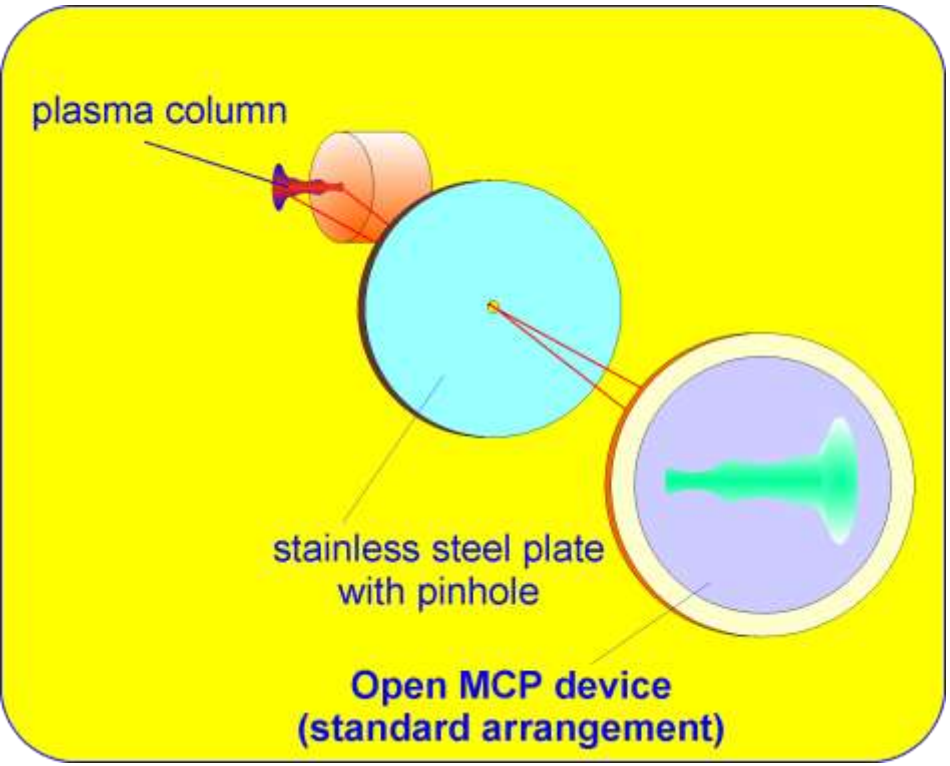

In standard solution of an open MCP-based device both MCP and a phosphor screen <u>are not divided</u> on electrically independent sectors

Design with Independent Sectors

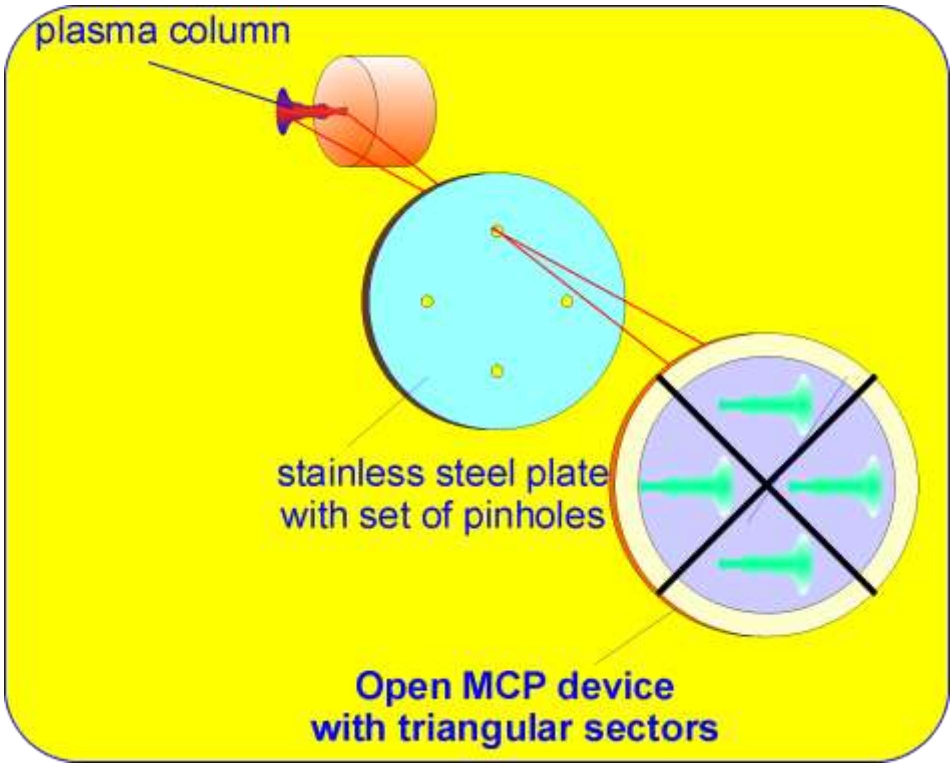

In this solution a phosphor screen <u>is divided</u> on electrically independent sectors

Different Arrangements of Open MCP-based Devices

Standard Design

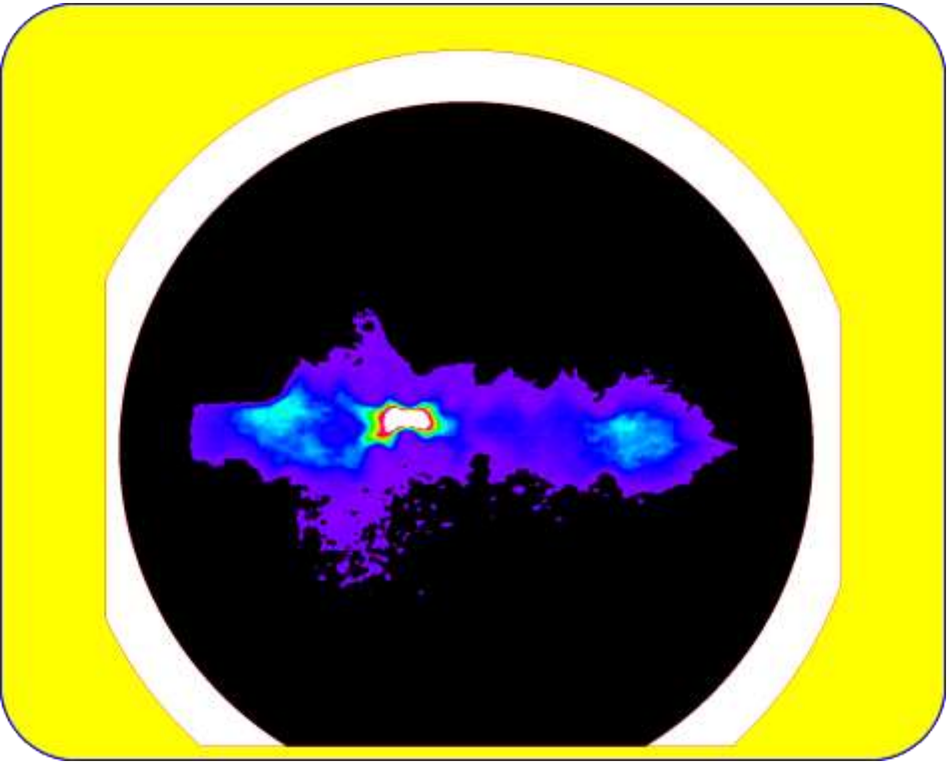

In standard solution of an open MCP-based device both MCP and a phosphor screen <u>are not divided</u> on electrically independent sectors

Design with Independent Sectors

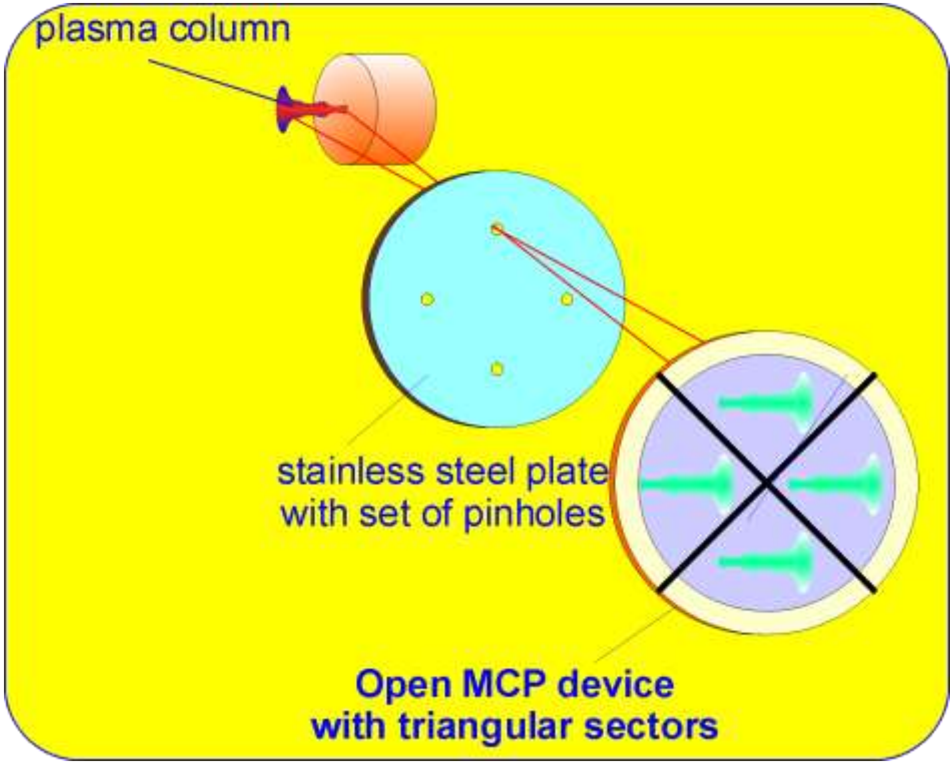

In this solution a phosphor screen <u>is divided</u> on electrically independent sectors

Images Recording in Different Spectral Range

Main Idea

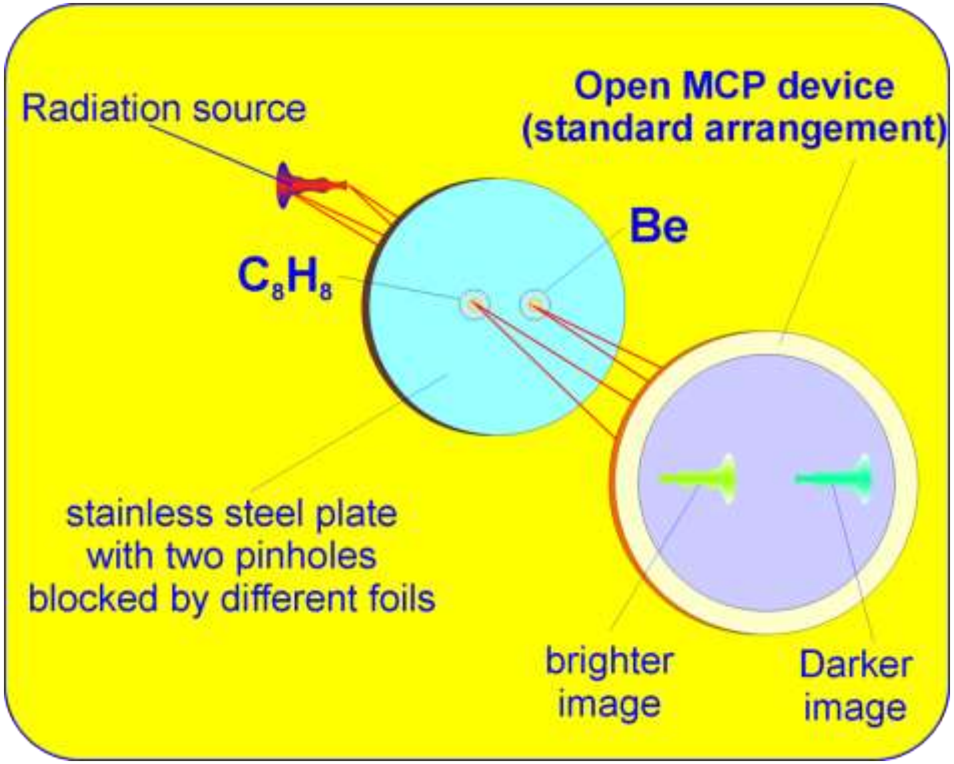

Subtraction of both images allows to obtain final image which constitute radiation emission in low energy spectral range

VUV-Soft X-ray Frame Camera

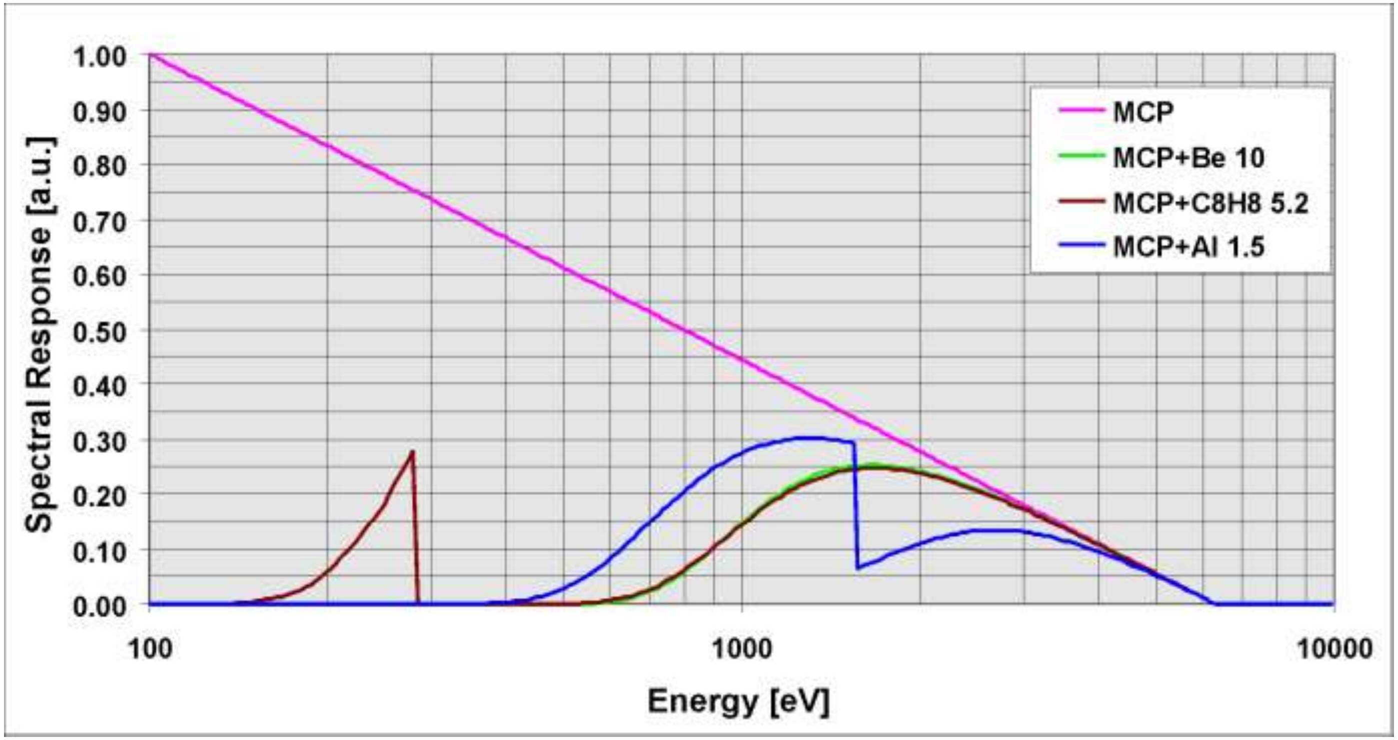

The blocking foil material and its thickness modify spectral response of whole camera arrangement.

Final Image Detector

- **High resolution CCD camera;**

  Resolution of 2048x2048x10 bits or 4096x4096x10 bits;
  Frame buffer capacity – enough to store about 512/128 frames;
  Frame rate – not higher than 6 fps;

- **CMOS high speed video camera;**

  Resolution from 1280x1024x8 bits to 128x128x8 bits;
  Frame buffer capacity – enough to store about 250000 frames;
  Frame rate – not higher than 20000 fps;

Final Image Detector

CMOS Cameras – High-Speed Video Technique (HSVT)

Total Number of Pixels versus Frame Rate

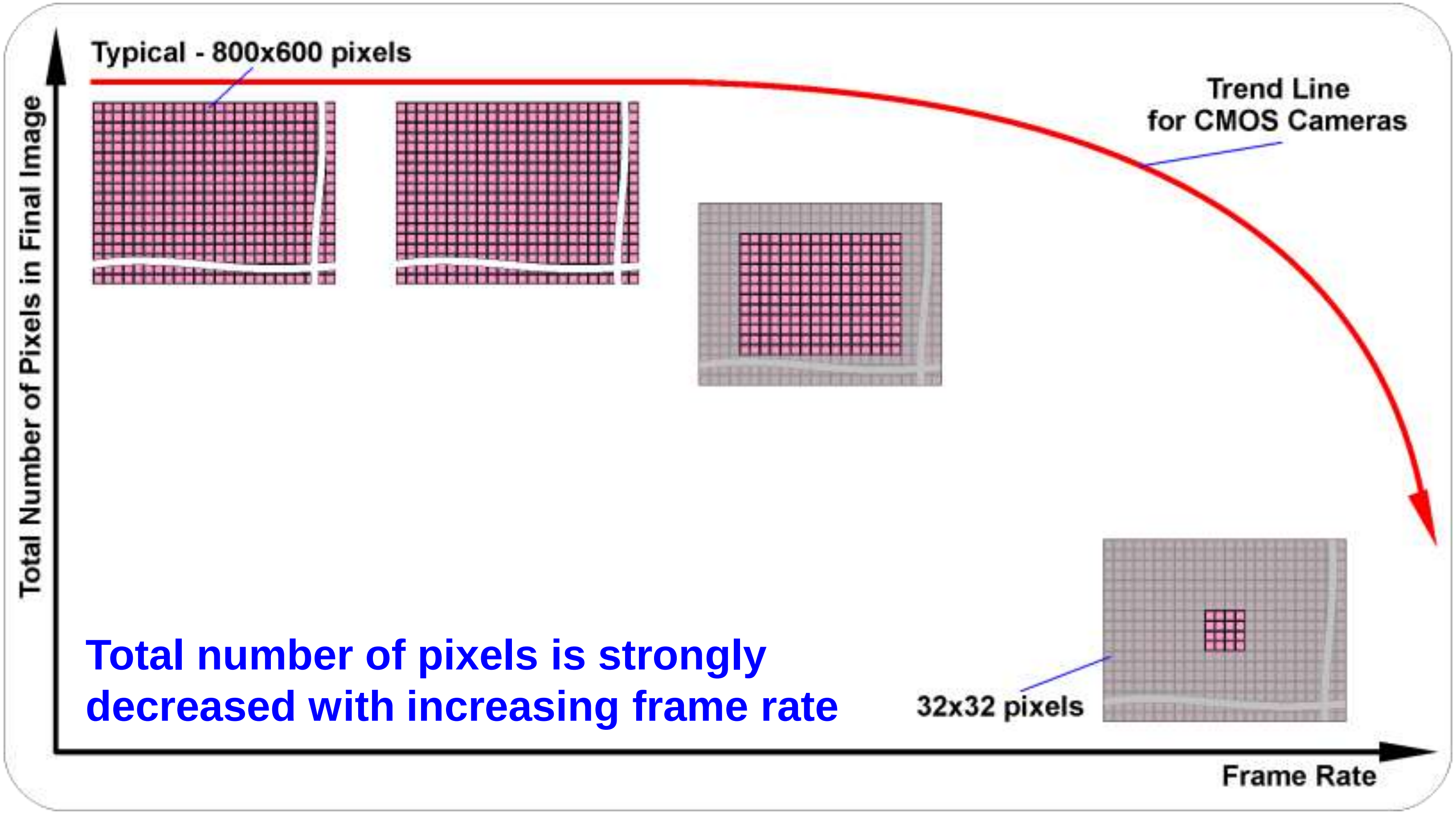

Expected Advantages

Proposed camera will be able to record images related to the behavior of the plasma itself and plasma wall interaction, as well as its evolution caused by externally-triggered processes (e.g. heating, pellet and plasma jet injection, etc.)

Such visualization (taken with high temporal and spatial resolution) will allow to:

- **Find the singularities of the internal plasma structure characterized by different radiance;**
- **Confirm of the occurrence of events predicted by plasma modeling or simulation codes;**
- **Unveil phenomena that could have been “hidden” so far;**